

Emulators for Large-scale Computer Experiments with Quantitative and Qualitative Inputs

Anita Shahrokhian¹, Youngdeok Hwang², and C. Devon Lin¹

¹Department of Mathematics and Statistics, Queen's University

²Paul H. Chook Department of Information Systems and Statistics, Baruch College, The City University of New York

Abstract

Computer experiments with both quantitative and qualitative inputs have become common across various areas. However, constructing accurate and computationally efficient emulators for such experiments at large scales remains a significant challenge. We propose a novel, scalable framework for emulating computer experiments with mixed inputs. Our approach is based on a new covariance function integrating additive Gaussian processes to handle the mixed inputs, with Vecchia approximation for scalability. We demonstrate that methods for large-scale computer experiments can be effectively extended when paired with our proposed modeling framework using simulation studies and a real structural engineering application.

Key Words: Big data, Gaussian process, Kriging, Surrogate, Uncertainty quantification, Vecchia approximation.

1 Introduction

Computer experiments have become an essential tool to drive new discovery and innovation across a wide spectrum of scientific and engineering, for combustion [Zhou et al. \(2025\)](#), system biology [Hwang et al. \(2025\)](#), energy storage [Escalante et al. \(2021\)](#), environment [Holthuijzen et al. \(2025\)](#), among many. These computer models allow researchers to overcome the inherent limitation of physical experiments, such as prohibitive costs, physical infeasibility, or ethical constraints [Gramacy \(2020\)](#).

Computer experiments increasingly involve mixed inputs, both quantitative and qualitative inputs, with wider applications of computer models of real-world systems (Shahrokhian et al., 2025). It is also a common practice to convert quantitative variables to a set of fixed values and treat them as qualitative variables when it is difficult to change the experimental settings. For instance, Qian et al. (2008)’s data center thermal flow case study had three qualitative factors, Deng et al. (2017) and Xiao et al. (2021) considered Young’s modulus of columns and other qualitative variables for embankments construction, and in the high-performance computing application studied by Cai et al. (2024) and Shahrokhian et al. (2025), Input/Output (IO) operation mode and IO scheduler are qualitative input variables.

With its increased importance and broader use, there have been efforts to incorporate mixed inputs in statistical surrogate models. A metric space needs to be introduced for qualitative variables using an appropriate covariance structure, such as a multiplicative form (Qian et al., 2008; Zhou et al., 2011) or an additive form (Deng et al., 2017; Xiao et al., 2021). When the number of qualitative variables increases, however, the computation becomes challenging because the number of covariance parameters increases rapidly. To keep the computation and estimation manageable, rigid assumptions are often placed on the covariance structure, which also adversarially affects the model performance.

The use of statistical emulators for large-scale computer experiments poses significant computational challenges. As dataset sizes grow, conventional Gaussian process (GP)-based approaches become computationally prohibitive, with computational and memory requirements scaling as $\mathcal{O}(n^3)$ and $\mathcal{O}(n^2)$, respectively, for n observations. The Vecchia approximation (Vecchia, 1988; Katzfuss et al., 2020) enables scalable estimation with faster likelihood evaluation for parameter inference in large datasets. Meanwhile, the abundance of data in massive datasets has allowed response surfaces to be modeled with localized structures, giving rise to methods such as the localized approximate GP (laGP, Gramacy and Apley, 2015) and TwinGP (Vakayil and Joseph, 2024).

Despite recent advances, scalable GP modeling for massive datasets with mixed inputs remains under-explored. Existing mixed-input emulation methods, such as the easy-to-interpret GPs (EzGPs) of Xiao et al. (2021) and latent variable GPs (LvGPs) of Zhang et al. (2020), offer flexible modeling frameworks for mixed inputs, but they face computational challenges when applied to large-scale datasets. To scale LvGPs, Yerramilli et al. (2023) proposed approximations for both the models and its fully Bayesian hyperparameter inference. They concluded that the Bayesian treatment offered limited benefits, though this was demonstrated only on small datasets (of size ≤ 100). On the other hand, Vecchia-based approximations and localized GP methods offer computationally affordable modeling, they have not yet been extended to handle mixed inputs. To bridge this gap, we introduce a

novel covariance function that incorporates qualitative factors into a computationally scalable framework. Our approach, building on recent advances, addresses the key challenges of modeling large-scale datasets with mixed inputs by enabling efficient prediction and full uncertainty quantification.

The remainder of this article is organized as follows. Section 2 provides a review of EzGP and associated methods, and the scaled Vecchia approximation. A new covariance function for mixed inputs is introduced in Section 3. Section 4 demonstrates how the proposed model adapts the two prominent methods for large-scale computer experiments. Section 5 presents several numerical studies to demonstrate the proposed method. Section 6 presents a case study with a real application in structural engineering. Section 7 concludes the paper.

2 Background

In this section, we review the methodologies that our approach is based upon. We first review the GP models for mixed inputs proposed by Xiao et al. (2021), followed by the scaled Vecchia approximation introduced by Katzfuss et al. (2022) for scalable analysis and emulation of large-scale computer experiments.

2.1 Easy-to-Interpret GP models

Consider a computer experiment with p quantitative variables $x^{(1)}, x^{(2)}, \dots, x^{(p)}$ and q qualitative factors $z^{(1)}, z^{(2)}, \dots, z^{(q)}$ where $z^{(h)}$ has m_h levels, for $h = 1, \dots, q$. Given the n responses y_1, \dots, y_n and n inputs $\mathbf{w}_1, \dots, \mathbf{w}_n$ where $\mathbf{w}_i = (\mathbf{x}_i^\top, \mathbf{z}_i^\top)^\top$, $\mathbf{x}_i = (x_{i1}, \dots, x_{ip})^\top$ and $\mathbf{z}_i = (z_{i1}, \dots, z_{iq})^\top$, to model the relationship between output Y and an input $\mathbf{w} = (\mathbf{x}^\top, \mathbf{z}^\top)^\top$, Xiao et al. (2021) proposed the model

$$Y(\mathbf{x}, \mathbf{z}) = \mu + G_0(\mathbf{x}) + G_{z^{(1)}}(\mathbf{x}) + \dots + G_{z^{(q)}}(\mathbf{x}), \quad (1)$$

where μ is a constant mean, G_0 and $G_{z^{(h)}}$'s are independent GPs with mean zero and covariance function ϕ_0 and ϕ_h , $h = 1, \dots, q$. Xiao et al. (2021) assumes that G_0 is a standard GP with only quantitative inputs \mathbf{x} in ϕ_0 given by,

$$\phi_0(\mathbf{x}_i, \mathbf{x}_j | \boldsymbol{\theta}^{(0)}) = \sigma_0^2 \exp\left\{-\sum_{k=1}^p \theta_k^{(0)} (x_{ik} - x_{jk})^2\right\}, \quad (2)$$

where all correlation parameters $\boldsymbol{\theta}^{(0)} = (\theta_1^{(0)}, \dots, \theta_p^{(0)})^\top$ are positive. For $h = 1, \dots, q$, the covariance function ϕ_h can be defined as

$$\phi_h((\mathbf{x}_i^\top, z_{ih})^\top, (\mathbf{x}_j^\top, z_{jh})^\top | \boldsymbol{\Theta}^{(h)}) = \sigma_h^2 \exp\left\{-\sum_{k=1}^p \theta_{kz_{ih}z_{jh}}^{(h)} (x_{ik} - x_{jk})^2\right\} \tau_{z_{ih}z_{jh}}^{(h)},$$

where $\theta_{kz_{ih}z_{jh}}^{(h)}$'s are the correlation parameters for the pair of levels z_{ih} and z_{jh} in $z^{(h)}$, $\tau_{z_{ih}z_{jh}}^{(h)}$ is the correlation between the two levels and σ_h^2 is the variance for $z^{(h)}$. This formulation leads to a large number of parameters and often suffers from computational challenges. To avoid this over-parametrization and improve the interpretability, [Xiao et al. \(2021\)](#) proposed a more efficient form of $G_{z^{(h)}}$ given by

$$\phi_h((\mathbf{x}_i^\top, z_{ih})^\top, (\mathbf{x}_j^\top, z_{jh})^\top | \boldsymbol{\Theta}^{(h)}) = \sum_{l_h=1}^{m_h} \sigma_h^2 \exp\left\{-\sum_{k=1}^p \theta_{kl_h}^{(h)} (x_{ik} - x_{jk})^2\right\} \mathbb{1}(z_{ih} = z_{jh} \equiv l_h), \quad (3)$$

where $\boldsymbol{\Theta}^{(h)} = (\theta_{kl_h}^{(h)})_{p \times m_h}$ is the matrix for the correlation parameters, and the indicator function is 1 when $z_{ih} = z_{jh} \equiv l_h$ and 0 otherwise for $l_h = 1, \dots, m_h$. Therefore, from (2) - (3), the covariance function for the model in (1) is given by

$$\begin{aligned} \phi(\mathbf{w}_i, \mathbf{w}_j) &= \text{Cov}(Y(\mathbf{w}_i), Y(\mathbf{w}_j)) = \phi_0(\mathbf{x}_i, \mathbf{x}_j | \boldsymbol{\theta}^{(0)}) + \sum_{h=1}^q \phi_h(\mathbf{x}_i, \mathbf{x}_j | \boldsymbol{\Theta}^{(h)}) \\ &= \sigma_0^2 \exp\left\{-\sum_{k=1}^p \theta_k^{(0)} (x_{ik} - x_{jk})^2\right\} \\ &\quad + \sum_{h=1}^q \sum_{l_h=1}^{m_h} \mathbb{1}(z_{ih} = z_{jh} \equiv l_h) \sigma_h^2 \exp\left\{-\sum_{k=1}^p \theta_{kl_h}^{(h)} (x_{ik} - x_{jk})^2\right\}. \end{aligned} \quad (4)$$

This covariance function has $2 + p + q + p \sum_{h=1}^q m_h$ parameters μ , σ_0^2 , $\theta_k^{(0)}$, σ_h^2 , and $\theta_{kl_h}^{(h)}$ for $h = 1, \dots, q$, $k = 1, \dots, p$ and $l_h = 1, \dots, m_h$, which can be estimated using the maximum likelihood estimation (MLE) method. Under the GP model in (1), the parameters can be found by minimizing the negative log-likelihood given by

$$\log |\boldsymbol{\Phi}| + (\mathbf{y} - \mu \mathbf{1}_n)^\top \boldsymbol{\Phi}^{-1} (\mathbf{y} - \mu \mathbf{1}_n), \quad (5)$$

with $\mathbf{y} = (y_1, \dots, y_n)^\top$, $\mathbf{1}_n$ being a vector of n ones, $\boldsymbol{\Phi} = (\phi(\mathbf{w}_i, \mathbf{w}_j))_{n \times n}$ with the covariance given in (4), after dropping the terms that are not dependent on the parameters. We denote the parameters in (4) by $\boldsymbol{\sigma}^2 = (\sigma_0^2, \dots, \sigma_q^2)^\top$, $\boldsymbol{\Theta} = (\boldsymbol{\theta}^{(0)}, \boldsymbol{\Theta}^{(1)}, \dots, \boldsymbol{\Theta}^{(q)})$ where $\boldsymbol{\theta}^{(0)} = (\theta_k^{(0)})_{p \times 1}$, and $\boldsymbol{\Theta}^{(h)} = (\theta_{kl_h}^{(h)})_{p \times m_h}$.

For a given σ^2 and Θ , the maximum likelihood estimate of μ is

$$\hat{\mu} = (\mathbf{1}_n^\top \Phi^{-1} \mathbf{1}_n)^{-1} \mathbf{1}_n^\top \Phi^{-1} \mathbf{y}, \quad (6)$$

and σ^2 and Θ can be obtained from

$$\{\hat{\sigma}^2, \hat{\Theta}\} = \underset{\sigma^2, \Theta}{\operatorname{argmin}} \{ \log |\Phi| + \mathbf{y}^\top \Phi^{-1} \mathbf{y} - (\mathbf{1}_n^\top \Phi^{-1} \mathbf{1}_n)^{-1} (\mathbf{1}_n^\top \Phi^{-1} \mathbf{y})^2 \},$$

using an optimization algorithm, such as `rgenoud` in R (Mebane, Jr. and Sekhon, 2011). Let $Y^* = Y(\mathbf{w}^*)$ denote the predicted Y at a new input \mathbf{w}^* . Given $\hat{\mu}$, $\hat{\sigma}^2$, and $\hat{\Theta}$, the predictive mean and the predictive variance at \mathbf{w}^* are

$$\begin{aligned} \mathbb{E}(Y^* | \mathbf{y}) &= \mu_* = \hat{\mu} + \mathbf{r}_0^\top \Phi^{-1} (\mathbf{y} - \hat{\mu} \mathbf{1}_n), \\ \operatorname{Var}(Y^* | \mathbf{y}) &= \sigma_*^2 = \sum_{i=0}^q \sigma_i^2 - \mathbf{r}_0^\top \Phi^{-1} \mathbf{r}_0 + \frac{(1 - \mathbf{1}_n^\top \Phi^{-1} \mathbf{r}_0)^2}{\mathbf{1}_n^\top \Phi^{-1} \mathbf{1}_n}, \end{aligned} \quad (7)$$

respectively, where \mathbf{r}_0 is the covariance vector of $\Phi(\mathbf{w}^*, \mathbf{w}_i)_{n \times 1}$ for $i = 1, \dots, n$. The covariance function of EzGP in (4) considers the distinct correlation parameters for $\theta_{klh}^{(h)}$ to scale the quantitative factors separately. To further simplify the computation, Xiao et al. (2021) proposed another covariance function called EEzGP, which uses a single correlation parameter $\theta_{lh}^{(h)}$ to scale all quantitative factors equally, rather than considering separate parameters for each quantitative factor. The covariance function for EEzGP is given by

$$\begin{aligned} \phi(\mathbf{w}_i, \mathbf{w}_j) &= \operatorname{Cov}(Y(\mathbf{w}_i), Y(\mathbf{w}_j)) \\ &= \sigma_0^2 \exp\left\{-\sum_{k=1}^p \theta_k (x_{ik} - x_{jk})^2\right\} \\ &\quad + \sum_{h=1}^q \sum_{l_h=1}^{m_h} \mathbb{1}(z_{ih} = z_{jh} \equiv l_h) \sigma_h^2 \exp\left\{-\sum_{k=1}^p \theta_{lh}^{(h)} (x_{ik} - x_{jk})^2\right\}. \end{aligned} \quad (8)$$

This model has $2 + p + q + \sum_{h=1}^q m_h$, which is much smaller than the number of parameters in the EzGP model.

However, both the EzGP and EEzGP models become computationally prohibitive for large n as these models have computational complexity of $O(n^3)$ and memory space complexity of $O(n^2)$ respectively with the training dataset size n . To mitigate this issue, Xiao et al. (2021) introduced the Localized EzGP (LEzGP) model, which works by selecting a sensible subset of training data for fitting the EEzGP or EzGP model conditional on a target input.

Consider an input vector $\mathbf{w} = (\mathbf{x}^\top, \mathbf{z}^\top)^\top$ and a target input $\mathbf{w}^* = (\mathbf{x}^{*\top}, \mathbf{z}^{*\top})^\top$. Let $N_z(\mathbf{w}, \mathbf{w}^*)$ denote the number of matching levels between the qualitative inputs \mathbf{z} and \mathbf{z}^* . For example, if $\mathbf{z} = (1, 2, 3)^\top$ and $\mathbf{z}^* = (3, 2, 1)^\top$, then $N_z(\mathbf{w}, \mathbf{w}^*) = 1$, since only the second level matches. The LEzGP model defines a tuning parameter n_s to be the minimum number of matching qualitative levels required for subset selection. Only inputs satisfying $N_z(\mathbf{w}, \mathbf{w}^*) \geq n_s$ are selected. For a given \mathbf{w}^* , this condition defines a subset of inputs with at least n_s matching qualitative levels. The choice of n_s is critical, as it directly influences the selection and the subset size. The following steps summarize the LEzGP model given the value of n_s :

1. For a target input \mathbf{w}^* , identify all inputs \mathbf{w}_i (where $i = 1, \dots, n$) that satisfy the matching criterion: $N_z(\mathbf{w}_i, \mathbf{w}^*) \geq n_s$. Denote this selected subset as \mathbf{K}_s .
2. Using the subset \mathbf{K}_s , apply either: the EzGP model in (4) or the EEzGP model in (8), to predict the response at the target input \mathbf{w}^* from Step 1.

For instance, consider an experiment with $p = 1$ and $q = 3$ each having 3 levels, where the design matrix is

$$\mathbf{w} = \begin{bmatrix} 0.5 & 1 & 1 & 1 \\ 0.6 & 3 & 2 & 3 \\ 0.7 & 2 & 1 & 3 \\ 0.8 & 2 & 2 & 3 \end{bmatrix},$$

and the target input $\mathbf{w}^* = (0.3, 1, 2, 3)^\top$. Let $n_s = 2$. The subset \mathbf{K}_s is selected such that at least n_s matching qualitative levels between each row of \mathbf{K}_s and the target input \mathbf{w}^* . Hence, both $(0.6, 3, 2, 3)^\top$ and $(0.8, 2, 2, 3)^\top$ will be selected for \mathbf{K}_s .

2.2 The Vecchia approximation

The Vecchia approximation is a computationally efficient method for approximating large covariance matrices in spatial statistics and GP modeling (Vecchia, 1988). By leveraging conditional independence in GP, it decomposes the joint likelihood into a product of low-dimensional conditional distributions, significantly reducing computational complexity from $\mathcal{O}(n^3)$ to approximately $\mathcal{O}(nm^2)$, where $m \ll n$ is the size of a carefully selected conditioning set. This approach has been extended to fast emulation for large-scale computer experiments by Katzfuss et al. (2022). They employed the Vecchia approximation to construct efficient emulators by transforming the input space, scaling each input variable according to its influence on the computer model’s responses.

Consider an n -run computer experiment with p quantitative variables. The data includes inputs $\mathbf{x}_i = (x_{i1}, \dots, x_{ip})^\top$ and the corresponding response $y_i = y(\mathbf{x}_i)$ for $i = 1, \dots, n$. Let $\mathbf{y} = (y_1, \dots, y_n)^\top$. Assume that \mathbf{y} follows a GP with mean μ , and covariance function $\mathbf{K} = (k(\mathbf{x}_i, \mathbf{x}_j))_{i,j=1,\dots,n}$. The Vecchia approximation approximates the joint density $p(\mathbf{y}) = \prod_{i=1}^n p(y_i|y_1, \dots, y_{i-1})$ by a product of univariate conditional densities, that is,

$$\hat{p}(\mathbf{y}) = \prod_{i=1}^n p(y_i|\mathbf{y}_{c(i)}), \quad (9)$$

where $c(i) \subset \{1, \dots, i-1\}$ is a conditioning index of size $|c(i)| = \min(m_s, i-1)$ for $i = \{2, \dots, n\}$ and m_s is the size of the conditioning set. [Katzfuss et al. \(2022\)](#) commented that a relatively small size of $m_s \ll n$ in (9) is sufficient for accurate approximation. Moreover, $p(y_i|\mathbf{y}_{c(i)})$ in (9) and all Gaussian distributions can be computed parallelly. The accuracy of the Vecchia approximation is influenced by the choice of ordering y_1, \dots, y_n and the selection of the conditioning sets $c(i)$'s. [Katzfuss et al. \(2022\)](#) demonstrated that high accuracy can be achieved using the maximum-minimum distance (maximin) ordering and the nearest-neighbor (NN) conditioning.

[Katzfuss et al. \(2022\)](#) introduced a scaled Vecchia approximation for fast emulation of computer models. They assume an anisotropic covariance function with a separate range parameter ξ_l for the l th input dimension known as automatic relevance determination, $K(\mathbf{x}_i, \mathbf{x}_j) = \tilde{K}(q(\mathbf{x}_i, \mathbf{x}_j))$ where

$$q(\mathbf{x}_i, \mathbf{x}_j) = \left(\sum_{l=1}^p \left(\frac{x_{il} - x_{jl}}{\xi_l} \right)^2 \right)^{1/2},$$

and \tilde{K} can be any covariance function that is valid (i.e., strictly positive definite) in R^p . The scaled Vecchia approximation applied the Vecchia approximation in a transformed input space, with each input scaled according to how strongly it relates to the computer-model response. That is, they use the scaled inputs

$$\tilde{\mathbf{x}} = \left(\frac{x^{(1)}}{\xi_1}, \dots, \frac{x^{(p)}}{\xi_p} \right), \quad (10)$$

where ξ_i 's are range parameters and $\frac{1}{\xi_l}$ is the relevance of the l th input dimension. By scaling the inputs using the estimated range parameters, this approach controls the effect of input variables on the model. The scaled Vecchia approximation considers a maximin ordering and the NN conditioning of the scaled $\tilde{\mathbf{x}}$, not the original \mathbf{x} . Denote the mean and

parameters including range parameters in the covariance in the scaled Vecchia approximation by μ and $\boldsymbol{\theta}$. To estimate the parameters, [Katzfuss et al. \(2022\)](#) used the Fisher scoring algorithm in [Guinness \(2021\)](#) by maximizing the logarithm of the Vecchia likelihood in (9). Consider the approximate log joint density $l(\mu, \boldsymbol{\theta}) = \log(\hat{p}_{\mu, \boldsymbol{\theta}})$, where $\hat{p}_{\mu, \boldsymbol{\theta}}$ is the Vecchia approximation in (9). Since computing the derivatives of the conditional densities in (9) can be computationally challenging, replacing them by the joint distribution leads to

$$l(\mu, \boldsymbol{\theta}) = \sum_{i=1}^n (\log p_{\mu, \boldsymbol{\theta}}(y_i, \mathbf{y}_{c(i)}) - \log p_{\mu, \boldsymbol{\theta}}(\mathbf{y}_{c(i)})). \quad (11)$$

This formulation leverages the gradient and Fisher information for the Gaussian distribution, both of which can be computed using standard formulas, starting from an initial value of $\boldsymbol{\theta}^{(0)}$ such that,

$$\boldsymbol{\theta}^{(k+1)} = \boldsymbol{\theta}^{(k)} + (\mathbf{M}^{(k)})^{-1} \mathbf{g}^{(k)}, \quad (12)$$

where $\mathbf{g}^{(k)} = \frac{\partial l(\mu, \boldsymbol{\theta})}{\partial \boldsymbol{\theta}}|_{\boldsymbol{\theta}=\boldsymbol{\theta}^{(k)}}$ and $\mathbf{M}^{(k)} = -E\{\frac{\partial^2 l(\mu, \boldsymbol{\theta})}{\partial \boldsymbol{\theta} \partial \boldsymbol{\theta}^\top}|_{\boldsymbol{\theta}=\boldsymbol{\theta}^{(k)}}\}$ are computed based on (11). The details of the estimation can be found in [Guinness \(2021\)](#). In [Katzfuss et al. \(2022\)](#), the Fisher scoring iterations change with $\tilde{\mathbf{x}}$ in (10). To speed up the process, the parameter estimates are only updated at every doubling step, i.e., $k = 2, 4, 8, \dots$

Given the estimated parameters, the Vecchia approximation provides predictions at unobserved inputs $\mathbf{x}_1^*, \dots, \mathbf{x}_{n_*}^*$ by applying the Vecchia approximation to the joint density of $\mathbf{y}^{\text{all}} = (\mathbf{y}, \mathbf{y}^*)$, where $\mathbf{y}^* = (y_1^*, \dots, y_{n_*}^*)^\top$ with $y_i^* = y(\mathbf{x}_i^*)$, $i = 1, \dots, n_*$. This approximation is used to accurately compute the posterior distribution of $\mathbf{y}^* = (y_1^*, \dots, y_{n_*}^*)^\top$ for large values of n_* . The posterior predictive distribution is

$$\hat{p}(\mathbf{y}^* | \mathbf{y}) = \prod_{i=1}^{n_*} p(y_i^* | \mathbf{y}_{g^*(i)}^{\text{all}}), \quad (13)$$

where $g^*(i)$ includes m_* points closes to y_i^* in terms of scaled distance among the points are previously ordered in \mathbf{y}^{all} .

3 A New Covariance Function

In this section, we propose extending the scaled Vecchia approximation of [Katzfuss et al. \(2022\)](#) to computer experiments with quantitative and qualitative inputs. The scaling method in [Katzfuss et al. \(2022\)](#) is carried out by multiplying each quantitative input variable \mathbf{x}_l by its relevance parameter $1/\xi_l$, which is estimated from the anisotropic covariance

function using Fisher scoring. A naive approach of extending the scaled Vecchia approximation to computer experiments with mixed inputs would be applying the scaling solely based on the covariance parameters associated with the quantitative inputs. In the case of EzGP or EEzGP, for example, one can scale the l th quantitative variable by $\sqrt{\theta_l^{(0)}}$ in (2). This approach, however, only accounts for relevance parameters in the model component that uses purely quantitative inputs, it inherently overlooks the influence of qualitative factors.

To address this issue and incorporate the effects of both quantitative and qualitative inputs, we propose the following covariance function for (1):

$$\begin{aligned}
K(\mathbf{w}_i, \mathbf{w}_j) &= \text{Cov}(Y(\mathbf{w}_i), Y(\mathbf{w}_j)) \\
&= \sigma_0^2 \exp\left\{-\sum_{k=1}^p \theta_k^{(0)} (x_{ik} - x_{jk})^2\right\} \\
&\quad + \sum_{h=1}^q \sum_{l_h=1}^{m_h} \mathbb{1}(z_{ih} = z_{jh} \equiv l_h) \sigma_h^2 \exp\left\{-\sum_{k=1}^p \theta_k (x_{ik} - x_{jk})^2\right\}.
\end{aligned} \tag{14}$$

In contrast to the covariance function in (4), we set $\theta_{kz_{ih}z_{jh}}^{(h)}$ in (4) to be θ_k . Our approach employs a GP that integrates both qualitative and quantitative inputs, but with correlation parameters that are invariant with respect to the qualitative variables. This constitutes a fundamental difference from the EEzGP covariance function in (8), which instead assumes that parameters are independent of those of quantitative variables. Consequently, the assumptions underlying the EEzGP model also render it incompatible with an extension of the scaled Vecchia approximation to handle mixed inputs.

The SEzGP model involves $2+2p+q$ parameters, μ , σ_0^2 , $\theta_k^{(0)}$, σ_h^2 , and θ_k , where $h = 1, \dots, q$ and $k = 1, \dots, p$. These parameters can be estimated using the MLE method as described in (5). The scaled Vecchia approximation is applied by using the scaled quantitative inputs $\tilde{\mathbf{x}} = (\sqrt{\theta_1}x^{(1)}, \sqrt{\theta_2}x^{(2)}, \dots, \sqrt{\theta_p}x^{(p)})^\top$ assuming that the standardized input space $[0, 1]^p$ for quantitative variables.

The analytical gradient expression to apply Fisher scoring in (12) is

$$-2 \frac{\partial l(\boldsymbol{\sigma}^2, \boldsymbol{\Theta})}{\partial \bullet} = \text{tr}(\mathbf{K}^{-1} \frac{\partial \mathbf{K}}{\partial \bullet}) - (\mathbf{y} - \hat{\boldsymbol{\mu}})^\top \mathbf{K}^{-1} \frac{\partial \mathbf{K}}{\partial \bullet} \mathbf{K}^{-1} (\mathbf{y} - \hat{\boldsymbol{\mu}}),$$

where $\boldsymbol{\sigma}^2 = (\sigma_0^2, \sigma_1^2, \dots, \sigma_q^2)$, $\boldsymbol{\Theta} = (\theta_1^{(0)}, \dots, \theta_p^{(0)}, \theta_1, \dots, \theta_p)$, with given $\hat{\boldsymbol{\mu}}$ in (6). Thus, for

the SEzGP covariance function in (14), and any $i, j = 1, \dots, n$,

$$\begin{aligned}\frac{\partial \mathbf{K}}{\partial \sigma_0^2} &= (\exp\{-\sum_{k=1}^p \theta_k^{(0)}(x_{ik} - x_{jk})^2\})_{n \times n}, \\ \frac{\partial \mathbf{K}}{\partial \sigma_h^2} &= (\sum_{l_h=1}^{m_h} \mathbb{1}(z_{ih} = z_{jh} \equiv l_h) \exp\{-\sum_{k=1}^p \theta_k(x_{ik} - x_{jk})^2\})_{n \times n}, \\ \frac{\partial \mathbf{K}}{\partial \theta_l^{(0)}} &= (-\sigma_0^2(x_{il} - x_{jl})^2 \exp\{-\sum_{k=1}^p \theta_k^{(0)}(x_{ik} - x_{jk})^2\})_{n \times n}, \\ \frac{\partial \mathbf{K}}{\partial \theta_l} &= (-\sum_{h=1}^q \sum_{l_h=1}^{m_h} \mathbb{1}(z_{ih} = z_{jh} \equiv l_h) \sigma_h^2(x_{il} - x_{jl})^2 \exp\{-\sum_{k=1}^p \theta_k(x_{ik} - x_{jk})^2\})_{n \times n}.\end{aligned}$$

Using the scaled quantitative inputs $\tilde{\mathbf{x}}$, the Vecchia likelihood in (11) can then be used to compute the gradient and the Fisher information matrix using the derivatives derived for the SEzGP covariance function. For the remainder of this paper, we call this method, which employs the scaled Vecchia approximation with the SEzGP covariance matrix, as SVA.

4 Extending laGP and TwinGP

This section introduces extensions of two prominent methods for large-scale computer experiments to handle mixed inputs. The first method is the localized approximate GP (laGP) model proposed by Gramacy and Apley (2015), and the second is the twinGP model introduced by Vakayil and Joseph (2024). These extensions are included as benchmark methods for comparison with the proposed approach.

4.1 Extending laGP

The laGP models (Gramacy and Apley, 2015) for fast emulation of large computer experiments use a family of sequential design schemes that dynamically define the support of a GP predictor based on a local subset of the data, and Gramacy and Apley (2015) further derived expressions for fast sequential updating of all needed quantities as the local designs are built up iteratively. More specifically, let \mathbf{X}_n be the n inputs in the training data, and let \mathbf{x}^* be the unobserved input for which the prediction will be made. Let $\mathbf{X}_m(\mathbf{x}^*) \subset \mathbf{X}_n$ be a set of m points near \mathbf{x}^* , where m is significantly smaller than n . For notational simplicity, we omit \mathbf{x}^* and denote the subset as \mathbf{X}_m . The selection process of the local design with m data points begins with an initial design of size n_0 . A convenient choice of the initial design is the nearest neighbor points close to \mathbf{x}^* . The follow-up points are selected via two design criteria, the mean squared prediction error (MSPE) and active learning Cohn (ALC),

aimed at enhancing prediction accuracy for each target test location by considering one step ahead and utilizing the currently available information (Gramacy and Apley, 2015). For $j = n_0, \dots, m - 1$, let \mathbf{D}_j be the data including the inputs and outputs at step j . The next input \mathbf{x}_{j+1} is sequentially selected and the design is updated as $\mathbf{D}_{j+1} = \mathbf{D}_j \cup (\mathbf{x}_{j+1}, y_{j+1})$. Given \mathbf{x}^* and the current design \mathbf{D}_j , the MSPE criterion selects the next input \mathbf{x}_{j+1} that maximizes

$$\begin{aligned} \text{MSPE}(\mathbf{x}_{j+1}, \mathbf{x}^*) &= E\{[\mathbf{Y}(\mathbf{x}^*) - \mu_{j+1}(\mathbf{x}^*; \hat{\boldsymbol{\theta}}_{j+1})]^2 | \mathbf{D}_j(\mathbf{x}^*)\} \\ &\approx V_j(\mathbf{x}^* | \mathbf{x}_{j+1}; \hat{\boldsymbol{\theta}}_j) + \left(\frac{\partial \mu_j(\mathbf{x}^*; \boldsymbol{\theta})}{\partial \boldsymbol{\theta}} \Big|_{\boldsymbol{\theta}=\hat{\boldsymbol{\theta}}_j}\right)^2 / G_{j+1}(\hat{\boldsymbol{\theta}}_j), \end{aligned} \quad (15)$$

where

$$V_j(\mathbf{x}^* | \mathbf{x}_{j+1}; \hat{\boldsymbol{\theta}}_j) = \frac{\psi_j}{j-2} v_{j+1}(\mathbf{x}^*; \hat{\boldsymbol{\theta}}_j),$$

with

$$\psi_j = \mathbf{Y}_j^\top \mathbf{K}_j^{-1} \mathbf{Y}_j, \quad \mathbf{Y}_j = (y_1, \dots, y_j)^\top,$$

and

$$v_{j+1}(\mathbf{x}^*; \hat{\boldsymbol{\theta}}_j) = \mathbf{K}_{j+1}(\mathbf{x}^*, \mathbf{x}^*) - \mathbf{k}_{j+1}^\top(\mathbf{x}^*) \mathbf{K}_{j+1}^{-1} \mathbf{k}_{j+1}(\mathbf{x}^*).$$

Furthermore, $\frac{\partial \mu_j(\mathbf{x}^*; \boldsymbol{\theta})}{\partial \boldsymbol{\theta}}$ denotes the derivative of the predictive mean at \mathbf{x}^* , given \mathbf{D}_j , with respect to $\boldsymbol{\theta}$, and $G_{j+1}(\hat{\boldsymbol{\theta}}_j)$ denotes the expected Fisher information matrix, which consists of the information from \mathbf{D}_j together with the expected contribution from the future observation y_{j+1} at \mathbf{x}_{j+1} . The analytic expressions for $\frac{\partial \mu_j(\mathbf{x}^*; \boldsymbol{\theta})}{\partial \boldsymbol{\theta}} \Big|_{\boldsymbol{\theta}=\hat{\boldsymbol{\theta}}_j}$ and $G_{j+1}(\hat{\boldsymbol{\theta}}_j)$ are provided in Gramacy and Apley (2015) and are omitted here for brevity.

The approximation proposed in (15) consists of two terms. The first term represents the updated predictive variance after augmenting \mathbf{D}_j with the candidate point \mathbf{x}_{j+1} , conditional on $\hat{\boldsymbol{\theta}}_j$. The second term accounts for the uncertainty arising from parameter estimation and involves two components: $\frac{\partial \mu_j(\mathbf{x}^*; \boldsymbol{\theta})}{\partial \boldsymbol{\theta}}$ which is the derivative of the predictive mean with respect to $\boldsymbol{\theta}$, and $G_{j+1}(\hat{\boldsymbol{\theta}}_j)$, which is the expected Fisher information matrix incorporating both the information from \mathbf{D}_j and the anticipated contribution from the future observation y_{j+1} at \mathbf{x}_{j+1} .

Gramacy and Apley (2015) discussed that when the Fisher information is large, the second term in (15) can be ignored and the criterion reduces to $V_j(\mathbf{x}^* | \mathbf{x}_{j+1}; \hat{\boldsymbol{\theta}}_j)$ that is the new variance at \mathbf{x}^* when \mathbf{x}_{j+1} is added to the design. In other words, the goal is to maximize the ALC criterion, and that can be updated from j to $j + 1$ quickly via partitioned inverse

equations by [Barnett \(1979\)](#) such that,

$$\begin{aligned} \text{ALC}(\mathbf{x}^*, \mathbf{x}_{j+1}) &= \mathbf{k}_{j+1}^\top(\mathbf{x}^*) \mathbf{g}_j(\mathbf{x}_j, \mathbf{x}_{j+1}) \mathbf{g}_j(\mathbf{x}_j, \mathbf{x}_{j+1})^\top v_j(\mathbf{x}_{j+1}) \mathbf{k}_{j+1}^\top(\mathbf{x}^*) \\ &\quad + 2\mathbf{k}_{j+1}^\top(\mathbf{x}^*) \mathbf{g}_j(\mathbf{x}_j, \mathbf{x}_{j+1}) \mathbf{K}(\mathbf{x}_{j+1}, \mathbf{x}^*) + \mathbf{K}(\mathbf{x}_{j+1}, \mathbf{x}^*)^2 / v_j(\mathbf{x}_{j+1}), \end{aligned} \quad (16)$$

where

$$\mathbf{g}_j(\mathbf{x}_j, \mathbf{x}_{j+1}) = \mathbf{K}_j^{-1} \mathbf{k}_j(\mathbf{x}_{j+1}) / v_j(\mathbf{x}_{j+1})$$

and

$$v_j(\mathbf{x}_{j+1}) = \mathbf{K}(\mathbf{x}_{j+1}, \mathbf{x}_{j+1}) - \mathbf{k}_j(\mathbf{x}_{j+1})^\top \mathbf{K}_j^{-1} \mathbf{k}_j(\mathbf{x}_{j+1}).$$

The mathematical details for both the MSPE and ALC criteria are thoroughly presented in [Gramacy and Apley \(2015\)](#). The fast update of the ALC criterion in (16) is computationally efficient when the MLE parameters are updated only once at the design’s final stage. These methods have been implemented in their R package `laGP` ([Gramacy, 2016](#)), which includes efficient routines for both the MSPE criterion (15) and the ALC criterion (16).

We extend the use of the ALC criterion in (16) to large-scale computer experiments with mixed inputs by incorporating the SEzGP model in (14). Specifically, our goal is to sequentially select \mathbf{w}_{j+1} that maximizes (16) using the covariance function in (14). We call this method as *La* for the remainder of this article.

The `laGP` package only supports isotropic covariance functions and is therefore not directly applicable to the SEzGP model. As a practical contribution, we implement the ALC criterion for SEzGP to extend the `laGP` framework to mixed-input settings, although the implementation is computationally slower because of the more complex covariance structure.

Similar to `laGP`, the predictive locations can be handled in parallel. For each test location \mathbf{w}^* , we start with n_0 initial design chosen by NN, and fix the MLE parameters, then employ the ALC criterion in (16) to select the next points adaptively. At the end of the adaptive design process, the MLE parameters are updated once, as recommended in `laGP`.

4.2 Extending TwinGP

The TwinGP approach proposed by [Vakayil and Joseph \(2024\)](#) enhances prediction in large-scale computer experiments by strategically selecting global and local points. The selection of global points remains independent of the specific locations to be predicted.

The TwinGP model’s correlation function combines two components: \mathbf{G} for g global points and \mathbf{L} for l local points, and it is,

$$\mathbf{R}(\mathbf{x}_a, \mathbf{x}_b) = (1 - \lambda) \mathbf{G}(\mathbf{x}_a, \mathbf{x}_b) + \lambda \mathbf{L}(\mathbf{x}_a, \mathbf{x}_b), \quad \lambda \in [0, 1], \quad (17)$$

where λ controls the proportion of the global and local points to build the correlation matrix \mathbf{R} . Let $m = g + l$, \mathbf{X}_n be the inputs in the training data, and $\mathbf{X}_m \subset \mathbf{X}_n$ be the chosen m points from the training data, then we have $\mathbf{G}_{mm} = \mathbf{G}(\mathbf{X}_m, \mathbf{X}_m)$ and $\mathbf{L}_{mm} = \mathbf{L}(\mathbf{X}_m, \mathbf{X}_m)$, and the correlation matrix for the m chosen points is

$$\mathbf{R}_{mm} = (1 - \lambda)\mathbf{G}_{mm} + \lambda\mathbf{L}_{mm}, \quad \lambda \in [0, 1].$$

For each predictive location \mathbf{x}^* , the g global points \mathbf{X}_g are chosen from \mathbf{X}_n via the Twinning approach, and the l local points \mathbf{X}_l are selected via the nearest-neighbor method from the remaining points $\mathbf{X}_n \setminus \mathbf{X}_g$. The selection of \mathbf{X}_l depends on \mathbf{x}^* , whereas \mathbf{X}_g is independent of the predictive location. The combined set of points for modeling is $\mathbf{X}_m(\mathbf{x}^*) = \mathbf{X}_g \cup \mathbf{X}_l$, hereafter denoted as \mathbf{X}_m for brevity. Let \mathbf{Y}_m be the response vector corresponding to \mathbf{X}_m , partitioned as $\mathbf{Y}_m = (\mathbf{Y}_g, \mathbf{Y}_l)$ for \mathbf{X}_g and \mathbf{X}_l , respectively. In addition, \mathbf{I}_m , \mathbf{I}_g , and \mathbf{I}_l represent identity matrices of dimensions $m \times m$, $g \times g$, and $l \times l$, respectively.

The predictive mean and predictive variance involve

$$\begin{aligned} \mathbf{R}_{mm} + \eta\mathbf{I}_m &= \begin{bmatrix} \mathbf{R}_{gg} + \eta\mathbf{I}_g & \mathbf{R}_{gl} \\ \mathbf{R}_{lg} & \mathbf{R}_{ll} + \eta\mathbf{I}_l \end{bmatrix}, \\ &= \begin{bmatrix} (1 - \lambda)\mathbf{G}_{gg} + \lambda\mathbf{L}_{gg} + \eta\mathbf{I}_g & (1 - \lambda)\mathbf{G}_{gl} + \lambda\mathbf{L}_{gl} \\ (1 - \lambda)\mathbf{G}_{lg} + \lambda\mathbf{L}_{lg} & (1 - \lambda)\mathbf{G}_{ll} + \lambda\mathbf{L}_{ll} + \eta\mathbf{I}_l \end{bmatrix}, \end{aligned} \quad (18)$$

where \mathbf{R}_{gg} is independent of the predictive location \mathbf{x}^* , implying that $[\mathbf{R}_{gg} + \eta\mathbf{I}_g]^{-1}$ can be predetermined beforehand. For a given \mathbf{x}^* , we have

$$[\mathbf{R}_{mm} + \eta\mathbf{I}_m]^{-1} = \begin{bmatrix} \Sigma_{gg}^{-1} + \Sigma_{gg}^{-1}\mathbf{R}_{gl}\mathbf{S}^{-1}\mathbf{R}_{lg}\Sigma_{gg}^{-1} & -\Sigma_{gg}^{-1}\mathbf{R}_{gl}\mathbf{S}^{-1} \\ -\mathbf{S}^{-1}\mathbf{R}_{lg}\Sigma_{gg}^{-1} & \mathbf{S}^{-1} \end{bmatrix}, \quad (19)$$

where $\Sigma_{gg} = \mathbf{R}_{gg} + \eta\mathbf{I}_g$ and $\mathbf{S} = \mathbf{R}_{ll} - \mathbf{R}_{lg}\Sigma_{gg}^{-1}\mathbf{R}_{gl}$. [Vakayil and Joseph \(2024\)](#) provided an approximation to estimate the parameters in \mathbf{R}_{ll} when the input variables are quantitative. This approximation, however, does not apply to the covariance function of EzGP, EEzGP, or SEzGP. Therefore, we introduce an extension of TwinGP for large-scale computer experiments with mixed inputs.

Our goal here is to select a subset of m training points \mathbf{W}_m from the training data \mathbf{W}_n . Similar to the TwinGP method, we consider \mathbf{W}_g as the set of global points selected using the Twinning method proposed by [Vakayil and Joseph \(2022\)](#). Then, for a given predictive location \mathbf{w}^* , the local points \mathbf{W}_l are identified using the nearest neighbor method. Before applying both the TwinGP method and the nearest neighbor method, we adopt one-hot

encoding to convert the qualitative variables into numeric formats. One-hot coding represents a categorical variable with k levels by k binary indicator variables, where exactly one variable takes the value 1 and the others take the value 0. For example, consider $p = 1, q = 2$, and with $m_1 = m_2 = 2$. Here we have 4 different level combinations, and hence by applying one-hot encoding for two-level qualitative variables, we have

$$(\mathbf{w}_1^\top, \mathbf{w}_2^\top, \mathbf{w}_3^\top, \mathbf{w}_4^\top)^\top = \begin{bmatrix} 0.5 & 1 & 1 \\ 0.6 & 1 & 2 \\ 0.7 & 2 & 1 \\ 0.8 & 2 & 2 \end{bmatrix} \Rightarrow \begin{bmatrix} 0.5 & 1 & 0 & 1 & 0 \\ 0.6 & 1 & 0 & 0 & 1 \\ 0.7 & 0 & 1 & 1 & 0 \\ 0.8 & 0 & 1 & 0 & 1 \end{bmatrix}.$$

This conversion is solely used for selecting the global points and the local points; the original form of the inputs is retained for all other parts of the modeling.

Let \mathbf{Y}_m represent the responses corresponding to \mathbf{W}_m , where $\mathbf{Y}_m = (\mathbf{Y}_g, \mathbf{Y}_l)$ corresponds to the responses for \mathbf{W}_g and \mathbf{W}_l , respectively. Although we are unable to use the Wendlands' compactly supported radial function and fast estimation approach for local points as done in [Vakayil and Joseph \(2024\)](#), we can apply the partitioned matrix approach proposed by [Barnett \(1979\)](#) to improve the computational efficiency. More specifically, the covariance matrix in (14) in the SEzGP models can be expressed as

$$\mathbf{K}_{mm} = \begin{bmatrix} \mathbf{K}_{gg} & \mathbf{K}_{gl} \\ \mathbf{K}_{gl}^\top & \mathbf{K}_{ll} \end{bmatrix}, \quad (20)$$

where \mathbf{K}_{gg} and \mathbf{K}_{ll} represent the covariance matrix for global points and local points, respectively. Applying the partitioned matrix approach, we have

$$\mathbf{K}_{mm}^{-1} = \begin{bmatrix} \mathbf{K}_{gg}^{-1} + \mathbf{g}_{gl}\mathbf{g}_{gl}^\top\nu_{gl} & \mathbf{g}_{gl} \\ \mathbf{g}_{gl}^\top & \nu_{gl}^{-1} \end{bmatrix}, \quad (21)$$

where $\mathbf{g}_{gl} = -\nu_{gl}^{-1}\mathbf{K}_{gg}^{-1}\mathbf{K}_{gl}$ and $\nu_{gl} = \mathbf{K}_{ll} - \mathbf{K}_{gl}^\top\mathbf{K}_{gg}^{-1}\mathbf{K}_{gl}$. Using this inverse decomposition, we can quickly update the negative log-likelihood in (5) such that,

$$l_m(\mu, \boldsymbol{\sigma}^2, \boldsymbol{\Theta}) = \log|\mathbf{K}_{gg}| + \log(\nu_{gl}) + (\mathbf{Y}_m - \mu_m\mathbf{1}_m)^\top \mathbf{K}_{mm}^{-1}(\mathbf{Y}_m - \mu_m\mathbf{1}_m), \quad (22)$$

where $\mu, \boldsymbol{\sigma}^2 = (\sigma_0^2, \sigma_1^2, \dots, \sigma_q^2)^\top$, and $\boldsymbol{\Theta} = (\boldsymbol{\theta}^{(0)}, \boldsymbol{\theta})$ are the mean, variances, and correlation parameters in (14), respectively. For each predictive location, \mathbf{K}_{mm}^{-1} in (21) is updated with

the corresponding local points. The estimate of μ_m is given by,

$$\hat{\mu}_m = (\mathbf{1}_m^\top \mathbf{K}_{mm}^{-1} \mathbf{1}_m)^{-1} (\mathbf{1}_m^\top \mathbf{K}_{mm}^{-1} \mathbf{Y}_m). \quad (23)$$

The negative log-likelihood function in (22) can be minimized given $\hat{\mu}_m$ in (23) to obtain $\hat{\sigma}^2$ and $\hat{\Theta}$ using an optimization algorithm such as `rgenoud` in R (Mebane, Jr. and Sekhon, 2011), such that,

$$\{\hat{\sigma}^2, \hat{\Theta}\} = \underset{\sigma^2, \Theta}{\operatorname{argmin}} \{ \log(\mathbf{K}_{gg}) + \log(\nu_{gt}) + (\mathbf{Y}_m^\top \mathbf{K}_{mm}^{-1} \mathbf{Y}_m) - (\mathbf{1}_m^\top \mathbf{K}_{mm}^{-1} \mathbf{1}_m)^{-1} (\mathbf{1}_m^\top \mathbf{K}_{mm}^{-1} \mathbf{Y}_m)^2 \}.$$

For computational efficiency, we parallelize the calculations across predictive locations using the `foreach` and `doParallel` packages in R (Daniel et al., 2022; Folashade Daniel et al., 2022). Our implementation leverages high-performance computing clusters provided by the Digital Research Alliance of Canada. We call this method as *Twin* for the remainder of this article.

5 Numerical Illustration

In this section, we conduct numerical experiments to evaluate the performance of the methods proposed in Sections 3 and 4. Specifically, we compare the following approaches:

- **SVA**: scaled Vecchia approximation using the SEzGP covariance function;
- **Twin**: an extension of TwinGP with the SEzGP covariance function;
- **La**: an extension of laGP with the SEzGP covariance function;
- **LE**: the LEzGP model equipped with the SEzGP covariance function;
- **VA**: non-scaled Vecchia approximation using the SEzGP covariance function;
- **NN**: A nearest-neighbor method combined with the SEzGP model, where neighbors are selected based on the Euclidean distance.

All compared methods employ the SEzGP covariance function. For further insight, Appendix A also evaluates their performance using the original EzGP covariance function, further demonstrating the superior performance of the SEzGP covariance function.

We examine two distinct scenarios:

- Scenario 1: Computer experiments with a sufficient number of points for each level combination of the qualitative input variables.

- Scenario 2: Computer experiments with a large number of level combinations, resulting from either more qualitative inputs or more levels per input, which leads to fewer design points allocated per level combination for the quantitative inputs.

Throughout the experiments, we use the following notation: n is the total run size, p and q denote the number of quantitative and qualitative input variables, respectively, and m is the size of the selected subdata. For method-specific parameters, m_s is the conditioning set size for VA, n_s is the tuning parameter in the LEzGP approach, and g and l represent the number of global and local points in Twin. As a guideline for tuning parameters, we adopt the sizes for global and local points (g and l) recommended by [Vakayil and Joseph \(2024\)](#) for Twin, and set $m_s = 1$ for $p = 1$ for VA following [Katzfuss et al. \(2022\)](#). After an empirical analysis of the performance, as illustrated in Figure 1 for [Example 1](#), we observe that the performance improves significantly up to $m_s = 5$, with diminishing returns beyond this point. Thus, we select $m_s \in \{2, \dots, 5\}$ for $p > 1$. While these settings may vary with problem specifics and data size, they prove effective for our experimental purposes. Guided by these principles, we establish the following specific configurations for each method:

- **Twin**: The size of global points is set to $g = \min\{50(p + q), \max\{\sqrt{n}, 10(p + q)\}\}$ and the size of local points is set to $l = \max\{25, 3(p + q)\}$.
- **La**: Starting with an initial set of $l = \max\{25, 3(p + q)\}$ points near \mathbf{w}^* chosen by the nearest neighbor method, 10 additional points are sequentially added based on the ALC criterion in [\(16\)](#).
- **LE**: The tuning parameter $n_s = q$ considered in the Scenario 1 and $n_s = q - 1$ in the Scenario 2.
- **NN**: The size of local points is set to $l = \max\{25, 3(p + q)\}$ plus 10 additional points.
- **SVA, VA**: The size of local points is set to $l = \max\{25, 3(p + q)\}$ plus 10 additional points. The conditioning set size m_s is set to 1 if $p = 1$, and between 2 and 5 if $p > 1$.

Table 1 summarizes the settings of the methods used in each of four examples.

The training data are generated as follows. A random Latin hypercube design (using the `randomLHS` function in the `lhs` package in R ([Carnell, 2024](#))) is used for choosing quantitative inputs, while qualitative inputs include all level combinations. To evaluate the performance of different methods, we compare the predicted responses and the true responses using the

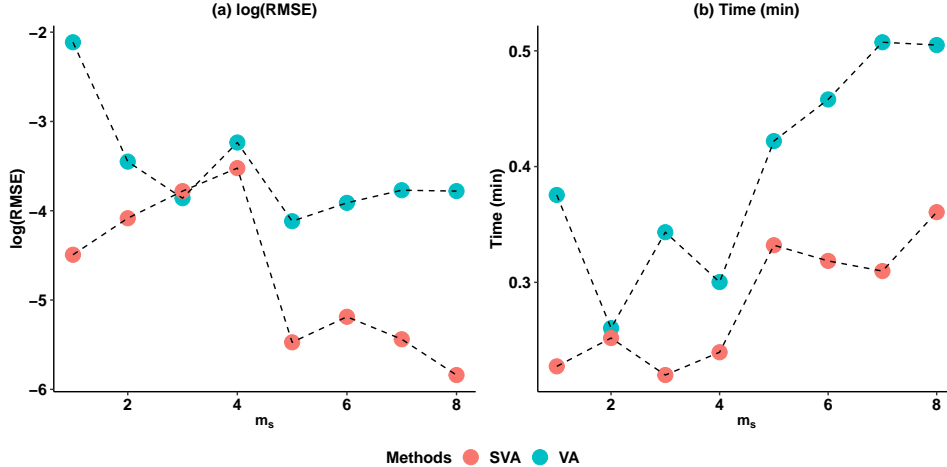


Figure 1: VA and SVA for $m_s = \{1, \dots, 8\}$ in Example 1: (a) log of RMSE; (b) time in minutes.

Example	Scenario	n	Twin (g, l, m)	NN/La (l, m)	VA/SVA (l, m, m_s)	LE (m, n_s)
Examples 1–2	Scenario 1	5400	$(80, 25, 105)$	$(25, 35)$	$(25, 35, 5)$	$(200, 3)$
Examples 1–2	Scenario 2	5000	$(73, 25, 98)$	$(25, 35)$	$(25, 35, 5)$	$(140, 2)$
Example 3	Scenario 1	5400	$(73, 25, 98)$	$(25, 35)$	$(25, 35, 3)$	$(200, 3)$
Example 4	Scenario 2	3645	$(71, 25, 96)$	$(25, 35)$	$(25, 35, 1)$	$(140, 5)$

Table 1: Summary of experimental configurations for each simulation scenario, with the total training points and the respective tuning parameters.

root mean square error (RMSE):

$$\text{RMSE} = \sqrt{\frac{1}{n_w} \sum_{i=1}^{n_w} \left(\hat{Y}(\mathbf{w}_i^*) - Y(\mathbf{w}_i^*) \right)^2}, \quad (24)$$

where n_w denotes the number of test points. The test set is constructed by first generating n_w points for quantitative inputs at each qualitative level combination via **randomLHS** (Carnell, 2024) and then randomly selecting n_w test locations from these points. This approach ensures random test location selection while maintaining a controlled test set size for fair comparison. In the captions of the figures in the examples, the values in the parenthesis represent the total size of the subdata in each method, and in the figures, we present the logarithm of the RMSE (base e). All the implementations can be found at https://github.com/devonlin/Emulator_for_large_mixed_inputs_computer_experiments.

Example 1

We consider a computer model with $p = 4$ quantitative inputs $\mathbf{x} = (x_1, x_2, x_3, x_4)$ and $q = 3$ qualitative inputs $\mathbf{z} = (z_1, z_2, z_3)$. The computer model is represented by,

$$f(\mathbf{x}, \mathbf{z}) = \frac{2\pi x_1 z_1}{\log(z_2/x_2)(1.5 + \frac{2x_3 x_1}{\log(z_2/x_2)x_2^2 z_3} + \frac{x_1}{x_4})}.$$

A similar function was considered by [Zhou et al. \(2011\)](#). The comparative setup and results for Scenarios 1 and 2 are discussed below.

- Scenario 1

We consider three levels for each qualitative input, yielding $3^3 = 27$ level combinations. The training data consists of 200 points per level combination and thus we have $200 \times 27 = 5400$ points in training data. The settings of all methods are summarized in Table 1. Figure 2 shows the log-RMSE and average computation time (in minutes) across 30 simulations for all methods using the SEzGP covariance function in (14). It also reveals that SVA achieves the lowest RMSE, demonstrating superior prediction accuracy among all methods. While NN offers the fastest computation time, it comes at the cost of significantly worse accuracy. Importantly, SVA maintains competitive computation times while delivering substantially better predictive performance, striking a balance between these two crucial metrics, making SVA the preferred choice.

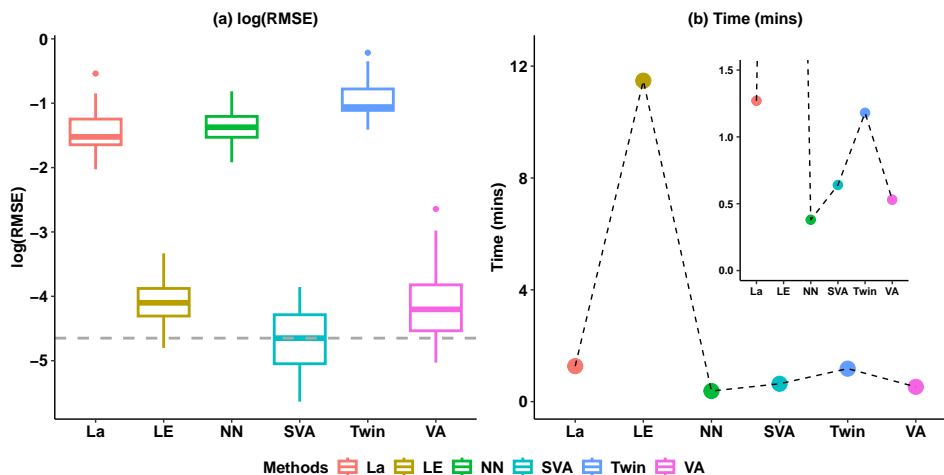


Figure 2: Simulation results for [Example 1](#), Scenario 1 across 30 replications: (a) The boxplot of log-RMSE; (b) The average of time in minutes, with Twin (105), LE (200), NN (35), La (35), VA (35) and SVA (35). The inset shows a zoomed-in view of plot (b).

- Scenario 2

We consider ten levels for each qualitative input variable, generating $10^3 = 1000$ level

combinations. The training dataset contains 5 points per level combination, totaling $5 \times 1000 = 5000$ points. The settings of all methods can be found in Table 1.

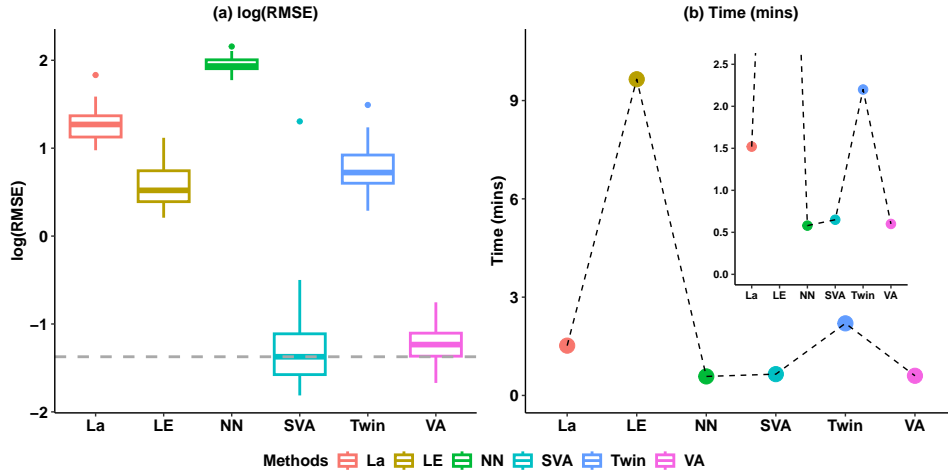


Figure 3: Simulation results for Example 1, Scenario 2 across 30 replications: (a) The boxplot of log-RMSE; (b) The average of time in minutes, with Twin (98), LE (140), NN (35), La (35), VA (35) and SVA (35).

Following the same approach as Scenario 1, Figure 3 displays the logarithm of the RMSE and average computation time (in minutes) across 30 simulations using the SEzGP covariance function in (14) in Scenario 2. The results demonstrate that SVA achieves superior prediction accuracy with the lowest RMSE values among all methods. While NN takes least computation time, its accuracy is significantly reduced. Again, SVA offers computational efficiency comparable to NN while delivering substantially better predictive performance. This superior accuracy-efficiency trade-off establishes SVA as the most practical and effective choice among the evaluated methods.

Example 2

We consider a computer model with 8 input variables in which, the five input variables x_1, \dots, x_5 are quantitative and the three inputs z_1, z_2, z_3 are qualitative. The computer model (An and Owen, 2001) is represented by,

$$\begin{aligned}
 u &= \sum_{i=1}^4 L_i \cos\left(\sum_{j=1}^i \theta_j\right) \\
 v &= \sum_{i=1}^4 L_i \sin\left(\sum_{j=1}^i \theta_j\right) \\
 f(\mathbf{w}) &= 10(u^2 + v^2)^{0.5},
 \end{aligned}$$

where $\mathbf{w} = (\theta_1, \theta_2, \dots, L_3, L_4)^\top$ with $\theta_1 = x_1, \theta_2 = x_2, \theta_3 = x_3, \theta_4 = x_4, L_1 = x_5, L_2 = z_1, L_3 = z_2, L_4 = z_3$. The setup and results for Scenarios 1 and 2 are as follows.

- Scenario 1

We consider three levels for each qualitative input, resulting $3^3 = 27$ level combinations. The training dataset consists of 200 points per level combination, resulting in a total of $200 \times 3^3 = 5400$ points. Figure 4 shows the log-RMSE and average computation time (in minutes) over 30 simulation runs for the six methods using the SEzGP covariance function in (14) under Scenario 1. Figure 4 reveals that the SVA method consistently achieves the lowest RMSE values and shorter computation times compared to the other methods, making it the most effective approach among the competitors.

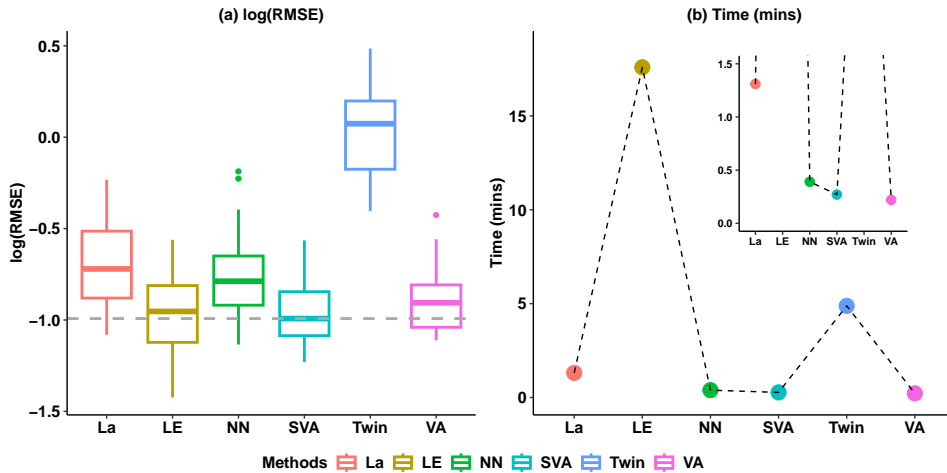


Figure 4: Simulation results for [Example 2](#) under Scenario 1 across 30 replications: (a) The boxplot of log-RMSE; (b) The average of time in minutes per simulation, with Twin (105), LE (200), NN (35), La (35), VA (35) and SVA (35).

- Scenario 2

We consider ten levels for each qualitative input variable, yielding $10^3 = 1000$ level combinations. The training dataset contains 5 points per level combination, totalling $5 \times 10^3 = 5000$ points. Figure 5 presents the log-RMSE and the average computation time (in minutes) across 30 simulations for the six methods, using the SEzGP covariance function in (14) under Scenario 2. Figure 5 reveals that while LE method achieves the lowest RMSE values, it incurs the highest computational cost. In contrast, SVA provides the second-best RMSE performance with substantially lower computation time. This shows that SVA offers a more favorable trade-off between accuracy and efficiency.

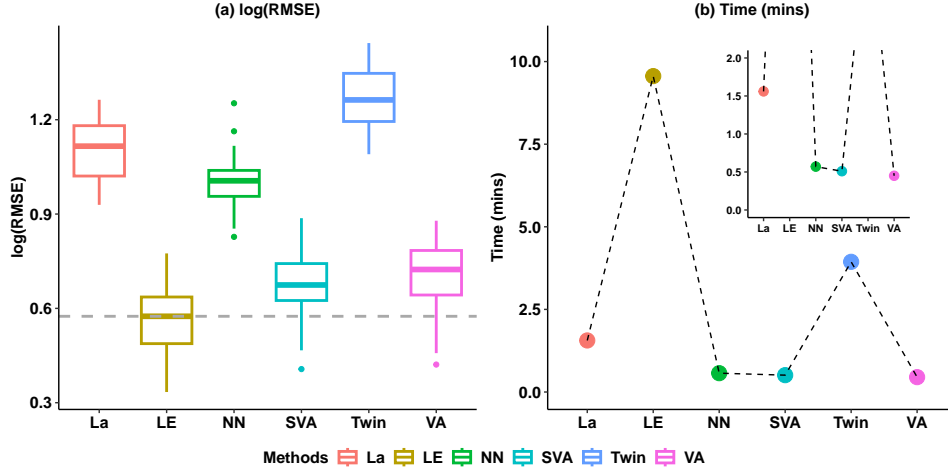


Figure 5: Simulation results for [Example 2](#), Scenario 2 across 30 replications: (a) The boxplot of log-RMSE; (b) The average of time in minutes, with Twin (105), LE (140), NN (35), La (35), VA (35) and SVA (35).

Example 3

We consider a computer model with $p = 3$ quantitative input variables $\mathbf{x} = (x_1, \dots, x_3)$ and $q = 3$ qualitative input variables $\mathbf{z} = (z_1, z_2, z_3)$. Following ([Xiao et al., 2021](#)), the function is defined as

$$i(\mathbf{x}, z_1) = \begin{cases} x_1 + x_2^2 + x_3, & \text{if } z_1 = 1 \\ x_1^2 + x_2 + x_3, & \text{if } z_1 = 2 \\ x_3 + x_1 + x_2^2, & \text{if } z_1 = 3, \end{cases} \quad g(\mathbf{x}, z_2) = \begin{cases} \cos(x_1) + \cos(2x_2) + \cos(x_3), & \text{if } z_2 = 1 \\ \cos(x_1) + \cos(2x_2) + \cos(x_3), & \text{if } z_2 = 2 \\ \cos(2x_1) + \cos(x_2) + \cos(x_3), & \text{if } z_2 = 3, \end{cases}$$

$$h(\mathbf{x}, z_3) = \begin{cases} \sin(x_1) + \sin(2x_2) + \sin(x_3), & \text{if } z_3 = 1 \\ \sin(x_1) + \sin(2x_2) + \sin(x_3), & \text{if } z_3 = 2 \\ \sin(2x_1) + \sin(x_2) + \sin(x_3), & \text{if } z_3 = 3, \end{cases} \quad f(\mathbf{x}, \mathbf{z}) = 100i(\mathbf{x}, z_1) + g(\mathbf{x}, z_2) + h(\mathbf{x}, z_3).$$

Due to the structure of this specific test function, increasing the number of levels for each qualitative variable to 10, as done in [Example 1](#) and [Example 2](#), is not feasible. As such, we limit our comparison for this example for Scenario 1.

We consider three levels for each qualitative input and thus we have $3^3 = 27$ level combinations in total. The training data consists of 200 points for each level combination, resulting in a total of $200 \times 3^3 = 5400$ points. [Figure 6](#) displays the log-RMSE and the average computation time (in minutes) across 30 simulations for the evaluated methods. The figure indicates that the SVA method consistently outperforms the other approaches in both prediction accuracy and computational efficiency. Specifically, SVA achieves lower RMSE values while requiring less computational time.

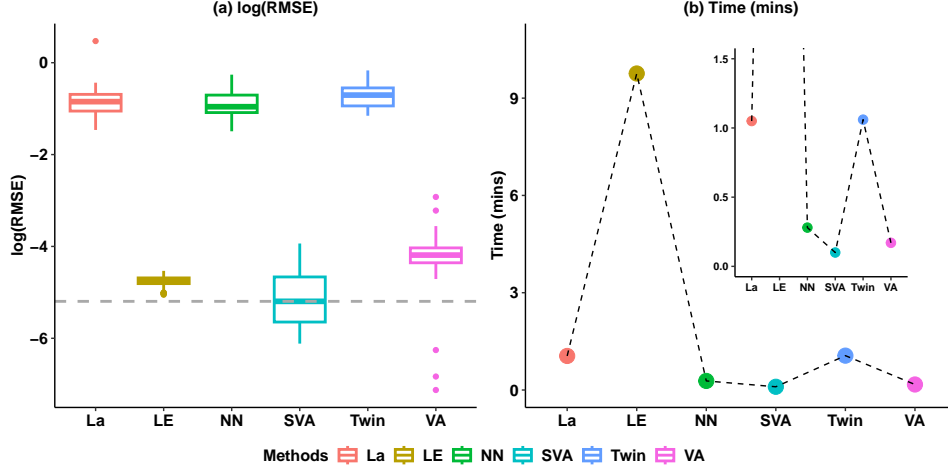


Figure 6: Simulation results for [Example 3](#) under Scenario 1 across 30 replications: (a) The boxplot of RMSE; (b) The average of time in minutes, with Twin (98), LE (200), NN (35), La (35), VA (35) and SVA (35).

Example 4

This example is designed to complement the results from [Example 3](#). This setup utilizes a similar class of functions but incorporates additional qualitative factors to create a larger-scale setting, to provide a more representative demonstration of the results when design points per level combination are limited. We consider a computer model with $p = 1$ quantitative input x and $q = 6$ qualitative inputs $\mathbf{z} = (z_1, z_2, z_3, z_4, z_5, z_6)$. The computer model is defined as

$$f(x, \mathbf{z}) = h(z_6) + e(z_5) + [\{(a(x, z_1) + b(x, z_2)) \cdot c(x, z_3) \cdot d(z_4)\},$$

where the functions $\{a, b, c, d, e, h\}$ are given by

$$a(x, z_1) = \begin{cases} \cos(3\pi x), & \text{if } z_1 = 1 \\ \cos(4\pi x), & \text{if } z_1 = 2 \\ \cos(5\pi x), & \text{if } z_1 = 3, \end{cases} \quad b(x, z_2) = \begin{cases} \sin(3\pi x), & \text{if } z_2 = 1 \\ \sin(4\pi x), & \text{if } z_2 = 2 \\ \sin(5\pi x), & \text{if } z_2 = 3, \end{cases} \quad c(z_3) = \begin{cases} 1, & \text{if } z_3 = 1 \\ 2, & \text{if } z_3 = 2 \\ 3, & \text{if } z_3 = 3, \end{cases}$$

$$d(z_4) = \begin{cases} 0.1, & \text{if } z_4 = 1 \\ 0.2, & \text{if } z_4 = 2 \\ 0.3, & \text{if } z_4 = 3, \end{cases} \quad e(x, z_5) = \begin{cases} x, & \text{if } z_5 = 1 \\ x^2, & \text{if } z_5 = 2 \\ x^3, & \text{if } z_5 = 3, \end{cases} \quad h(z_6) = \begin{cases} -2, & \text{if } z_6 = 1 \\ 0, & \text{if } z_6 = 2 \\ 2, & \text{if } z_6 = 3. \end{cases}$$

We now present the comparison framework and results for Scenario 2. We consider three levels for each qualitative input and thus there are a total of $3^6 = 729$ level combinations. The training data consists of 5 points per level combination, resulting in a total of $5 \times 3^6 = 3645$ data points. Figure 7 displays the log-RMSE and the average computation time (in minutes) across 30 simulations for the evaluated methods. Figure 7 reveals that the SVA method consistently outperforms the other approaches in both prediction accuracy and computational efficiency. Specifically, SVA achieves lower RMSE values, making it the most efficient method overall. It is worth pointing out the SVA significantly outperforms the VA in this example, highlighting the advantage of scaled framework.

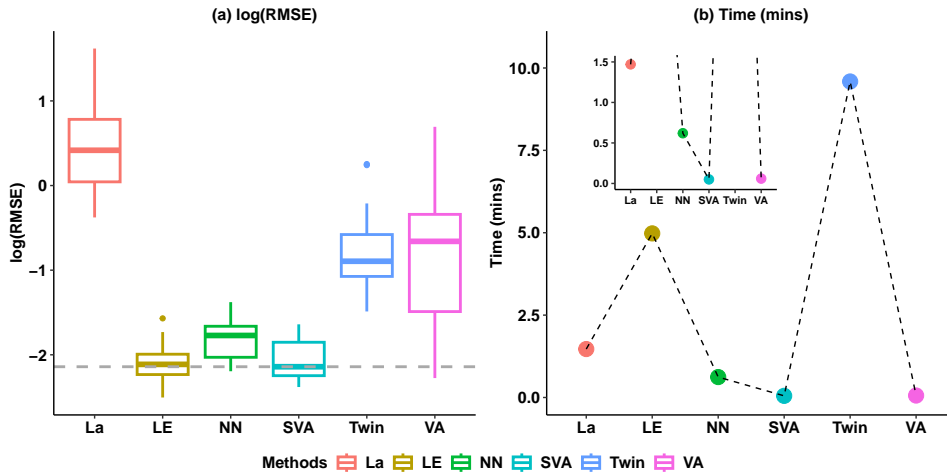


Figure 7: Simulation results for Example 4 under Scenario 2 across 30 replications: (a) The boxplot of RMSE; (b) The average of time in minutes, with Twin (96), LE (65), NN (35), La (35), VA (35) and SVA (35).

6 A Real Application

In this section, we present a case study to evaluate the predictive and computational performance of the methods, motivated by an engineering application. Specifically, we focus on beam deflection, a primary response metric used in structural engineering to prevent cracking and ensure overall system stability. To create a realistic dataset, we synthesized beam deflection cases by incorporating the geometries from the American Institute of Steel Construction (AISC) shapes database (American Institute of Steel Construction, 2013). The continuous inputs involved in the physical process are the depth and the cross-sectional area of the beam, the span length, and the load position along the beam. This simulation is based on a physics model that calculates the maximum deflection of a simply-supported beam subjected to a point load of unit magnitude. The magnitude of deflection is governed by the

beam’s physical geometric properties, material properties (i.e., the modulus of elasticity), and the location of the applied load.

To ensure the synthesized cases strictly follow physical constraints and simulate realistic behaviors, we used the W-shape (H-beam) geometric configurations from the AISC database as a baseline. For the comparative study, dimensions for other cross-sections, such as circular, rectangular shapes, and T-sections, were synthesized to be physically comparable to the actual geometries found in the AISC database. For each geometric configuration, values for the remaining quantitative inputs, span length and load position ratio, were sampled using a maximin Latin hypercube design. Two qualitative inputs are materials (four levels: steel, aluminum, concrete and wood) and cross sections (five levels: rectangular shape with two width-to-height ratios, circular, T-shapes, and H-shapes). The complete specification of the input parameters and the response variable is summarized in Table 2. The training data consist of 8,000 runs based on 20 geometric conditions and 20 combinations of length and load positions across all five shapes and four materials. Similarly, the test data consist of 2,000 runs generated from 100 geometric conditions and one combination of length and load positions for each of 30 simulation replications. In this case study, the LE method was excluded from the comparison due to its prohibitive computational cost.

Variable Type	Variables	Description
Quantitative	Beam Length	Maximin design
	Load Ratio	Maximin design
	Area	AISC Database
	Depth	AISC Database
Qualitative	Material	Steel, Aluminum, Concrete, Wood
	Shape	H-shape, T-shape, Circular, Rect (1:2), Rect (1:4)
Response	Maximum Deflection	Simulated via physics-based model

Table 2: Variable specifications for the large-scale beam deflection case study, detailing both the input parameters and the response variable.

Figure 8 presents the log-RMSE and the average computation time (in minutes) across 30 simulations for the five methods. As shown in Figure 8, the SVA method generally outperforms the other approaches in both predictive accuracy and computational efficiency.

7 Concluding Remarks

In this work, we investigated several techniques for large-scale computer experiments involving both quantitative and qualitative inputs. In particular, we proposed a novel scaled Vecchia approximation method, termed SEzGP, for such experiments, as described in Section 3. We also extended two prominent methods for large-scale computer experiments with

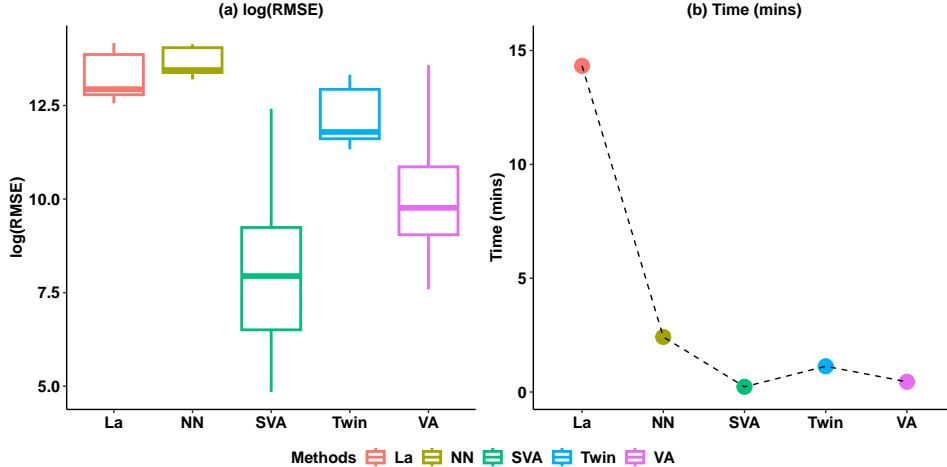


Figure 8: Performance comparison across 30 simulations for the case study: (a) boxplots of log-RMSE; (b) average computation time in minutes. The values in parentheses represent the number of points used for modeling for each method: Twin (89), NN (25), La (35), VA (35), and SVA (35).

quantitative inputs, laGP and TwinGP, to accommodate mixed-input settings.

Vecchia approximations employ an ordered conditional representation that enables efficient joint likelihood estimation, prediction, and uncertainty quantification. The proposed SEzGP method incorporates scaling parameters that automatically capture the effects of both quantitative and qualitative inputs through a fast parameter estimation procedure. By leveraging the advantages of Vecchia approximations, the proposed approach improves both predictive accuracy and computational efficiency for computer experiments with mixed inputs. Numerical studies and a real-data application demonstrate that the proposed method consistently outperforms competing approaches, including La, Twin, NN, LE, and VA, across a variety of large-scale computer experiment settings. Although our extensions of laGP and TwinGP did not exhibit the same advantages as observed in large-scale computer experiments with only quantitative inputs, more sophisticated extensions may further reveal their potential for the mixed-input settings.

In this study, the EzGP framework was used to construct the surrogate model. Other frameworks for mixed inputs, such as LvGP (Zhang et al., 2020) and category tree GP (Lin et al., 2024), are also worth investigating in the context of large-scale computer experiments. For future research, we plan to investigate the use of the proposed covariance function in inference tasks, such as global optimization and contour estimation for large-scale computer experiments with mixed inputs.

Acknowledgment

Lin was supported by a Discovery grant from the Natural Sciences and Engineering Research Council of Canada. Part of this research was performed while Hwang and Lin were visiting the Institute for Mathematical and Statistical Innovation (IMSI) at University of Chicago from March 3 to May 24, 2025, which is supported by the National Science Foundation (Grant No. DMS-1929348). We also thank Digital Research Alliance of Canada for providing clusters for computing.

Appendix

A Comparison of EzGP and SEzGP

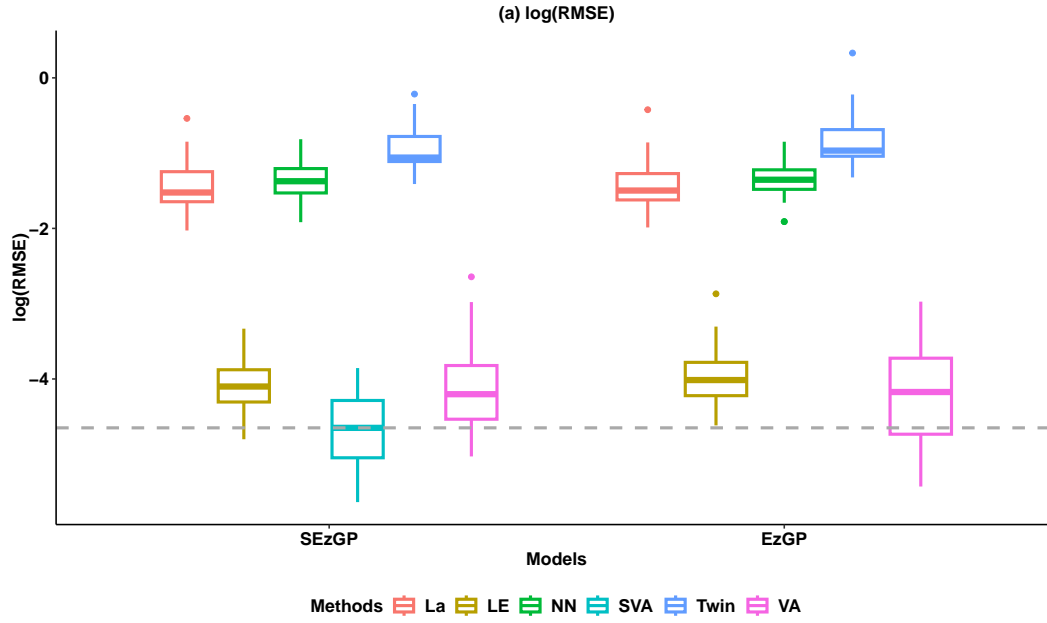
We compare the prediction accuracy and computational efficiency of different methods for large-scale computer experiments involving both quantitative and qualitative inputs. In particular, we focus on the EzGP and SEzGP covariance functions. The motivation for these comparisons is to highlight the performance advantages of the SEzGP covariance function, defined in (14), over the standard EzGP covariance function.

The SEzGP covariance function not only yields more accurate predictions - as evidenced by lower RMSE values - but also significantly reduces the computational time required for model fitting and prediction. Figures 9 through 14 show the logarithm of the RMSE and the average computational time (in minutes) for both covariance functions.

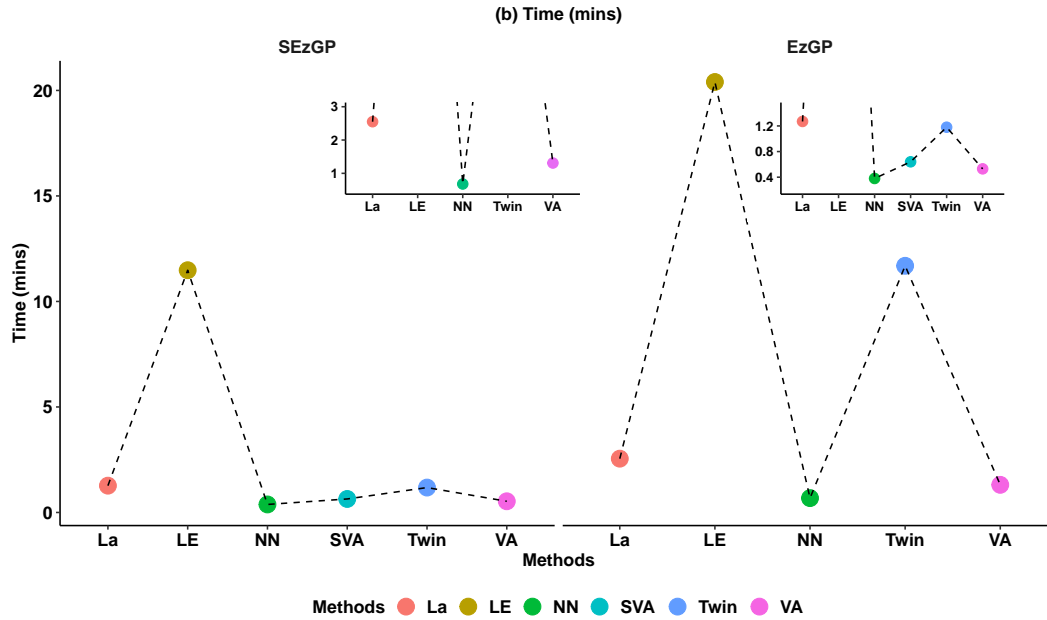
These results demonstrate that SEzGP consistently achieves a better trade-off between predictive accuracy and computational efficiency, making it a more suitable choice for large-scale computer experiments with mixed-inputs.

References

- American Institute of Steel Construction (2013). AISC shapes database v14.1. <https://www.aisc.org>.
- An, J. and A. Owen (2001). Quasi-regression. *Journal of Complexity* 17(4), 588–607.
- Barnett, S. (1979). Matrix methods for engineers and scientists. *McGraw-Hill*.
- Cai, X., L. Xu, C. D. Lin, Y. Hong, and X. Deng (2024). Adaptive-region sequential design with quantitative and qualitative factors in application to HPC configuration. *Journal of Quality Technology* 56(1), 5–19.



(a)

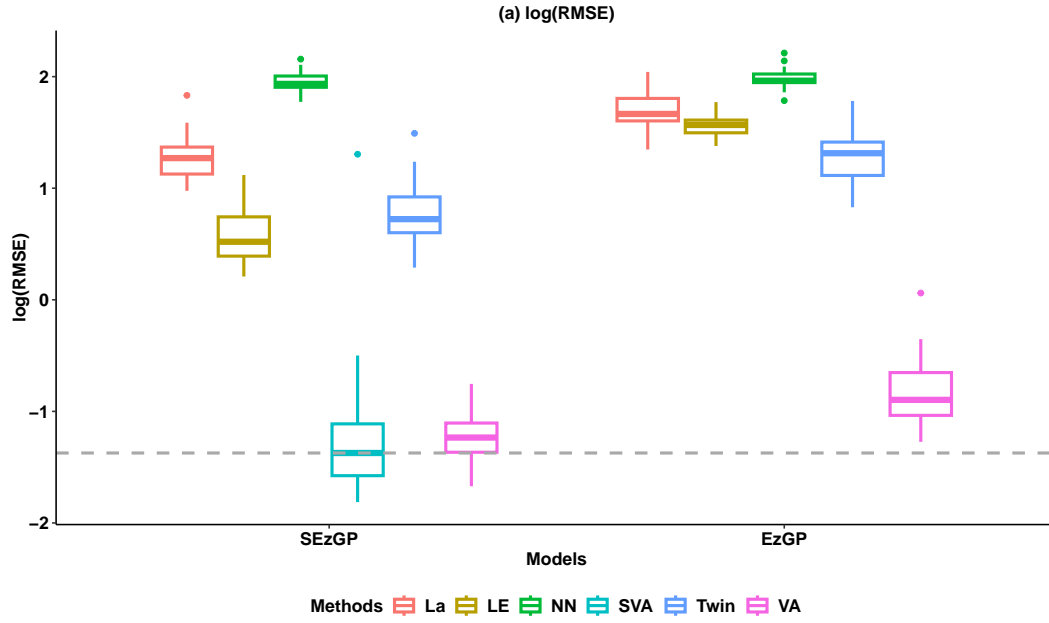


(b)

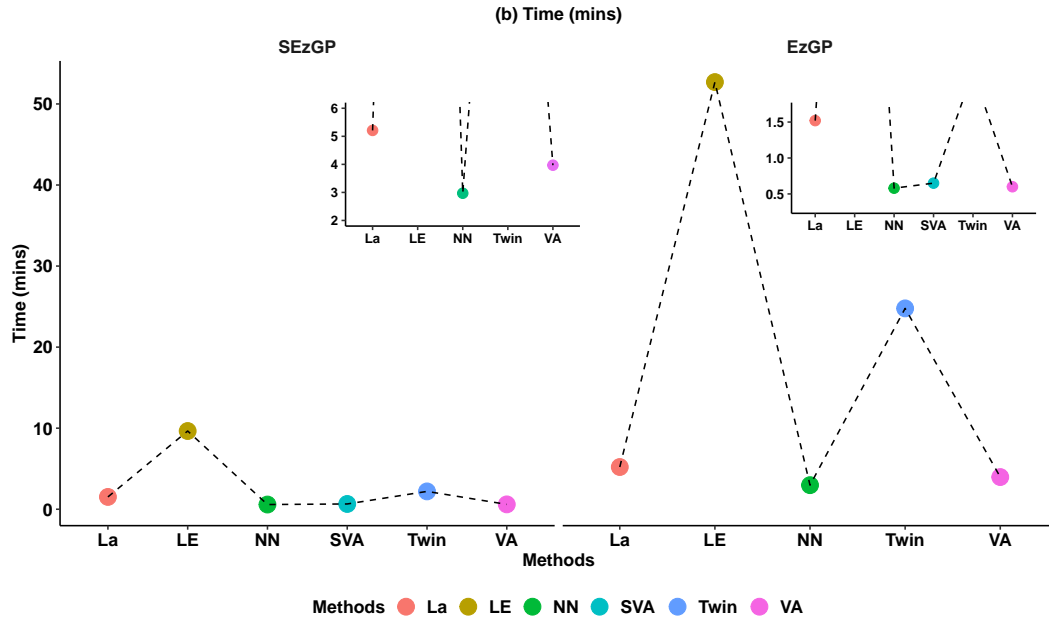
Figure 9: (a) Boxplot of RMSE values; (b) Average computation time in minutes for Twin (105), LE (200), NN, La, VA, and SVA (35) methods, using EzGP and SEzGP across 30 simulations in [Example 1](#), Scenario 1.

Carnell, R. (2024). *lhs: Latin Hypercube Samples*. R package version 1.2.0.

Daniel, F., H. Ooi, R. Calaway, M. Corporation, and S. Weston (2022). *foreach: Provides*



(a)



(b)

Figure 10: (a) RMSE boxplot; (b) Average computation time (minutes) for Twin (98), LE (140), NN, La, VA, and SVA (35) methods using SEzGP across 30 simulations in Scenario 2 of [Example 1](#).

Foreach Looping Construct. R Foundation for Statistical Computing.

Deng, X., C. D. Lin, K.-W. Liu, and R. Rowe (2017). Additive Gaussian process for computer models with qualitative and quantitative factors. *Technometrics* 59(3), 283–292.

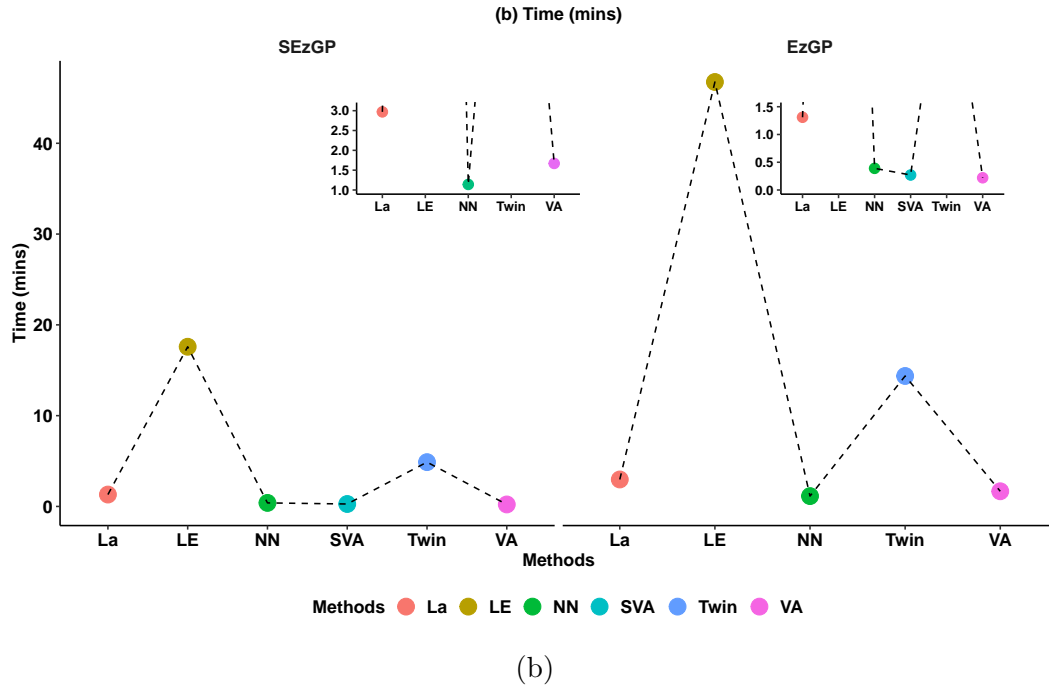
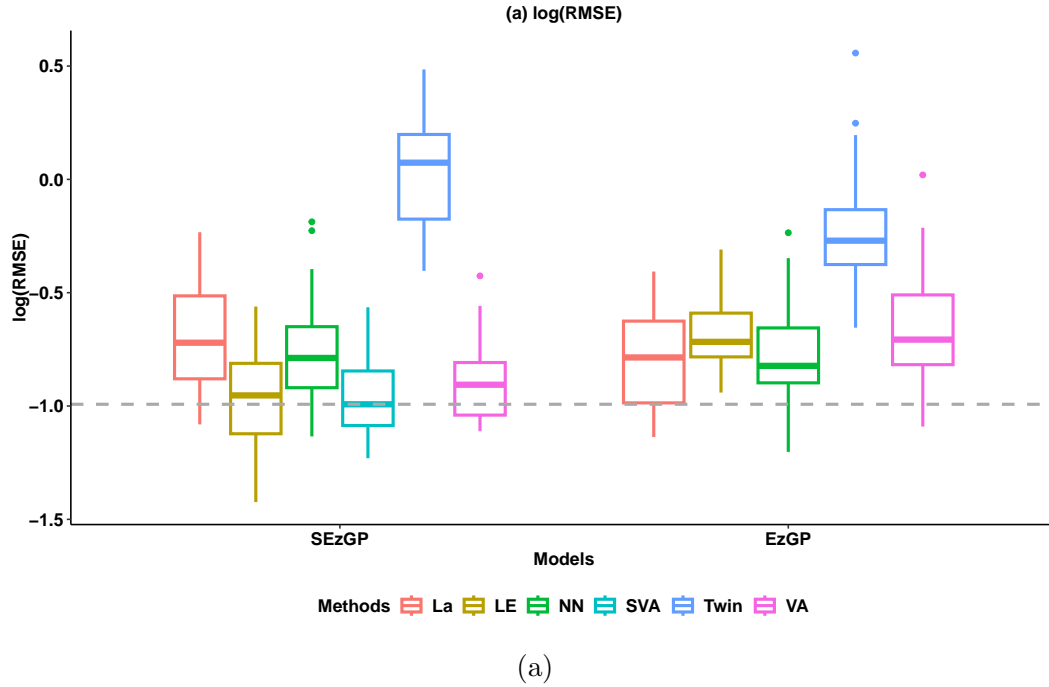
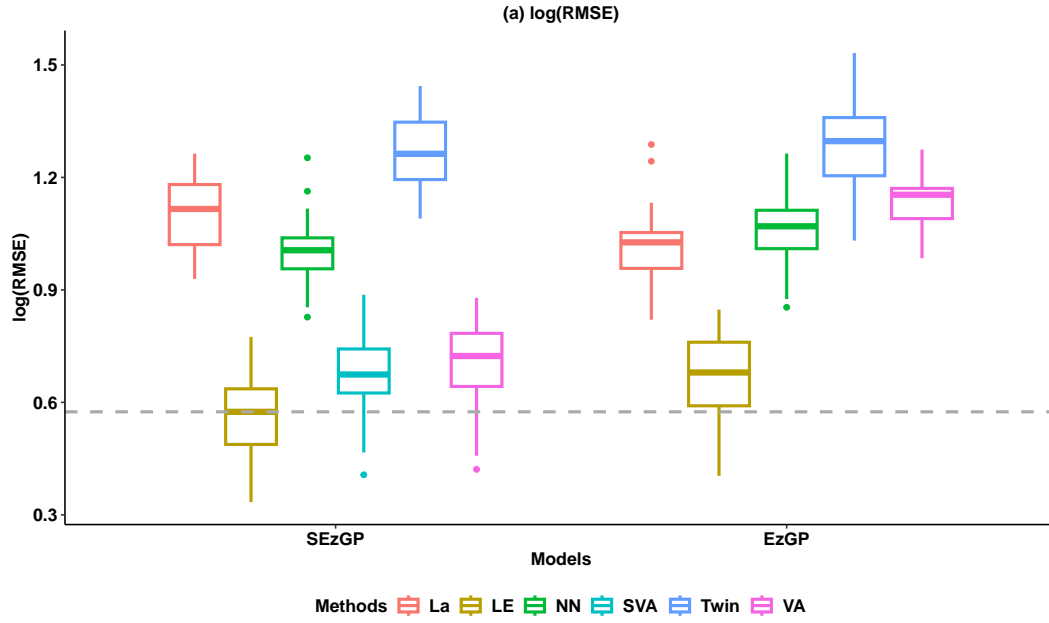
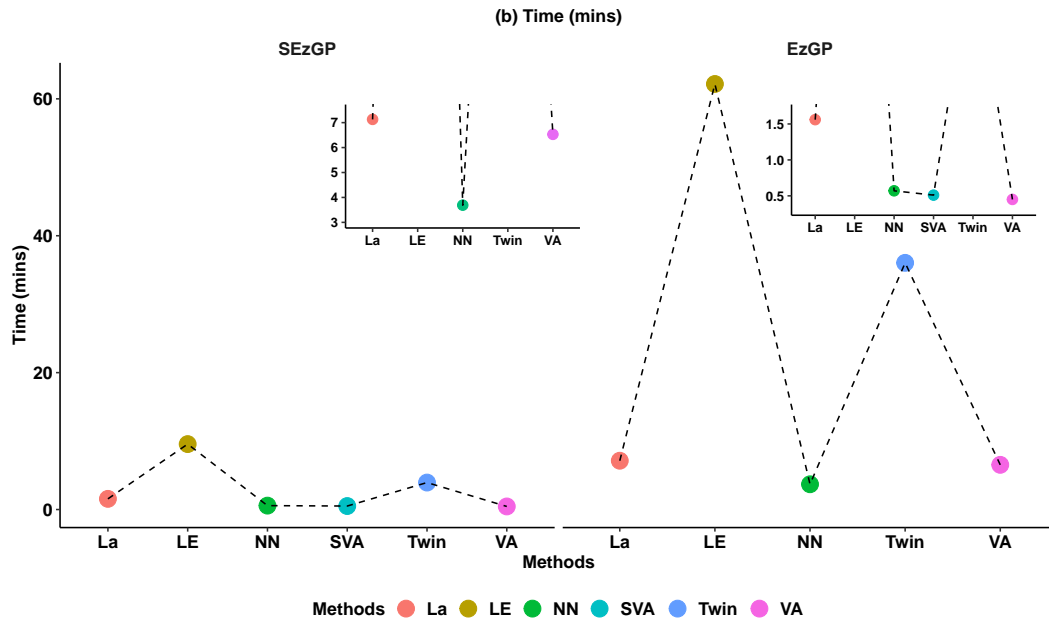


Figure 11: (a) RMSE boxplot; (b) Average computation time (minutes) for Twin (105), LE (200), NN, La, VA, and SVA (35) methods using EzGP and SEzGP across 30 simulations in Scenario 1 of [Example 2](#).

Escalante, J. M., S. Sahu, J. M. Foster, and B. Protas (2021). On uncertainty quantification in the parametrization of newman-type models of lithium-ion batteries. *Journal of The Electrochemical Society* 168(11), 110519.



(a)

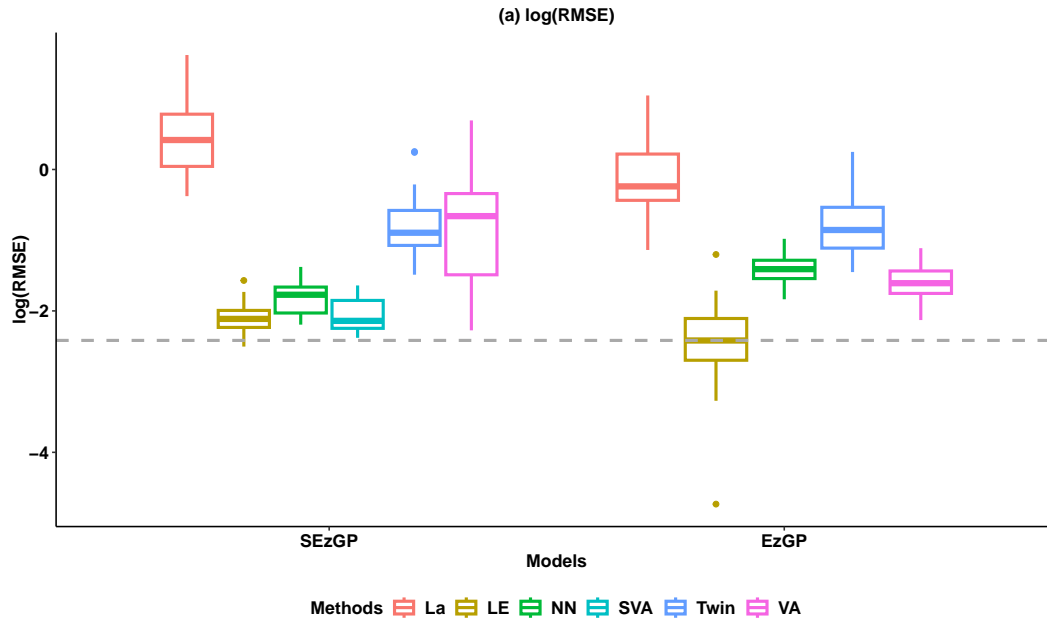


(b)

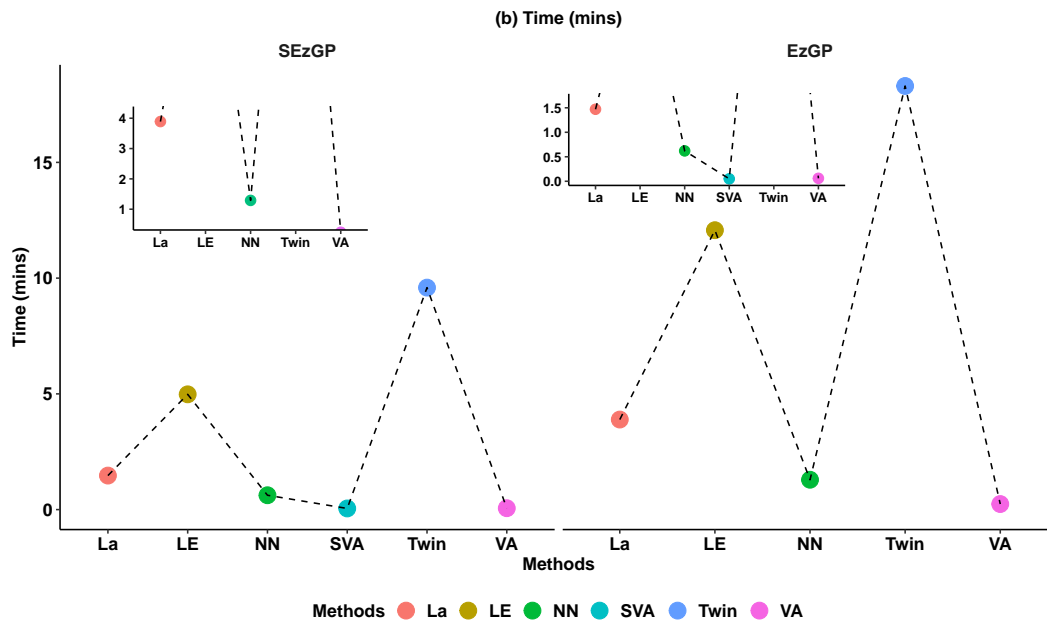
Figure 12: (a) RMSE boxplot; (b) Average computation time (minutes) for Twin (105), LE (140), NN, La, VA, and SVA (35) methods using EzGP and SEzGP across 30 simulations in Scenario 2 of [Example 2](#).

Folashade Daniel, M. C., S. Weston, and D. Tenenbaum (2022). *doParallel: Foreach Parallel Adaptor for the 'parallel' Package*. R Foundation for Statistical Computing.

Gramacy, R. B. (2016). laGP: large-scale spatial modeling via local approximate Gaussian



(a)



(b)

Figure 14: (a) RMSE boxplot; (b) Average computation time (minutes) for Twin (96), LE (65), NN, La, VA, and SVA (35) methods using EzGP and SEzGP across 30 simulations in Scenario 2 of Example 4.

gramacy.com/surrogates/.

Gramacy, R. B. and D. W. Apley (2015). Local Gaussian process approximation for large computer experiments. *Journal of Computational and Graphical Statistics* 24(2), 561–578.

- Guinness, J. (2021). Gaussian process learning via Fisher scoring of Vecchia’s approximation. *Statistics and Computing* 31(3), 25–32.
- Holthuijzen, M. F., R. B. Gramacy, C. C. Carey, D. M. Higdon, and R. Q. Thomas (2025). Synthesizing data products, mathematical models, and observations for lake temperature forecasting. *The Annals of Applied Statistics* 19(2), 1127–1146.
- Hwang, Y., H. J. Kim, W. Chang, C. Hong, and S. N. M. and (2025). Bayesian model calibration and sensitivity analysis for oscillating biological experiments. *Technometrics* 67(2), 333–343.
- Katzfuss, M., J. Guinness, W. Gong, and D. Zilber (2020). Vecchia approximations of Gaussian process predictions. *Journal of Agricultural, Biological and Environmental Statistics* 25, 383–414.
- Katzfuss, M., J. Guinness, and E. Lawrence (2022). Scaled Vecchia approximation for fast computer-model emulation. *SIAM/ASA Journal on Uncertainty Quantification* 10(2), 537–554.
- Lin, W.-A., C.-L. Sung, and R.-B. Chen (2024). Category tree Gaussian process for computer experiments with many-category qualitative factors and application to cooling system design. *Journal of Quality Technology* 56(5), 391–408.
- Mebane, Jr., W. R. and J. S. Sekhon (2011). Genetic optimization using derivatives: The rgenoud package for R. *Journal of Statistical Software* 42(11), 1–26.
- Qian, P. Z. G., H. Wu, and C. J. Wu (2008). Gaussian process models for computer experiments with qualitative and quantitative factors. *Technometrics* 50(3), 383–396.
- Shahrokhian, A., X. Deng, and C. D. Lin (2025). Active learning of computer experiment with both quantitative and qualitative inputs. *Statistics in Industry and Government* 53, 129–159.
- Shahrokhian, A., X. Deng, C. D. Lin, P. Ranjan, and L. Xu (2025). Adaptive design for contour estimation from computer experiments with quantitative and qualitative inputs. *SIAM/ASA Journal on Uncertainty Quantification* 13(4), 1766–1790.
- Vakayil, A. and V. R. Joseph (2022). Data twinning. *Statistical Analysis and Data Mining: The ASA Data Science Journal* 15(5), 598–610.

- Vakayil, A. and V. R. Joseph (2024). A global-local approximation framework for large-scale Gaussian process modeling. *Technometrics* 66(2), 295–305.
- Vecchia, A. V. (1988). Estimation and model identification for continuous spatial processes. *Journal of the Royal Statistical Society Series B: Statistical Methodology* 50(2), 297–312.
- Xiao, Q., A. Mandal, C. D. Lin, and X. Deng (2021). EzGP: Easy-to-interpret Gaussian process models for computer experiments with both quantitative and qualitative factors. *SIAM/ASA Journal on Uncertainty Quantification* 9(2), 333–353.
- Yerramilli, S., A. Iyer, W. Chen, and D. W. Apley (2023). Fully bayesian inference for latent variable Gaussian process models. *SIAM/ASA Journal on Uncertainty Quantification* 11(4), 1357–1381.
- Zhang, Y., S. Tao, W. Chen, and D. W. Apley (2020). A latent variable approach to Gaussian process modeling with qualitative and quantitative factors. *Technometrics* 62(3), 291–302.
- Zhou, M., R. Zuo, C.-L. Sung, Y. Tong, and X. Wang (2025). Region-optimal gaussian process surrogate model via dirichlet process for cold-flow and combustion emulations. *Computer Methods in Applied Mechanics and Engineering* 439, 117894.
- Zhou, Q., P. Z. Qian, and S. Zhou (2011). A simple approach to emulation for computer models with qualitative and quantitative factors. *Technometrics* 53(3), 266–273.